2001

Molding Large Area Plastic Parts Covered With HARMs.

Mircea Stefan Despa
Louisiana State University and Agricultural & Mechanical College

INFORMATION TO USERS

This manuscript has been reproduced from the microfilm master. UMI films the text directly from the original or copy submitted. Thus, some thesis and dissertation copies are in typewriter face, while others may be from any type of computer printer.

The quality of this reproduction is dependent upon the quality of the copy submitted. Broken or indistinct print, colored or poor quality illustrations and photographs, print bleedthrough, substandard margins, and improper alignment can adversely affect reproduction.

In the unlikely event that the author did not send UMI a complete manuscript and there are missing pages, these will be noted. Also, if unauthorized copyright material had to be removed, a note will indicate the deletion.

Oversize materials (e.g., maps, drawings, charts) are reproduced by sectioning the original, beginning at the upper left-hand corner and continuing from left to right in equal sections with small overlaps.

Photographs included in the original manuscript have been reproduced xerographically in this copy. Higher quality 6" x 9" black and white photographic prints are available for any photographs or illustrations appearing in this copy for an additional charge. Contact UMI directly to order.

ProQuest Information and Learning
300 North Zeeb Road, Ann Arbor, MI 48106-1346 USA
800-521-0600

MOLDING LARGE AREA PLASTIC PARTS COVERED WITH HARMS

A Dissertation

Submitted to the Graduate Faculty of
Louisiana State University and
Agricultural and Mechanical College
In partial fulfillment of the
requirements for the degree of
Doctor of Philosophy

in

The Interdepartmental Program in Engineering

by
Mircea S. Despa
B.S. in Chemical Engineering, UPB Bucharest, Romania, 1994
M.S. in Chemical Engineering, LSU, May 1998
May 2001

To the memory of my mother

ACKNOWLEDGEMENTS

I wish to express my gratitude to Dr. Kevin Kelly for his help and guidance. I thank him for his advice and for his continuous challenge; I became a better person through both. Also, I want to thank my wife, Simona, for her advice with statistical issues, and more important, for her immense support and patience. Paul Rodriguez and Ron Bouchard were instrumental with their input in the design, manufacture, and imaging of devices and parts.

TABLE OF CONTENTS

ABSTRACT

Injection molding and hot embossing proved to be suitable for use to reproduce layouts of micropatterns manufactured by LIGA. The research work was based on two commercially available machines. Preliminary experiments with both machines indicated that several modifications and additions were necessary to adapt the injection machine and the embossing press for microreplication. For the injection machine, a mold geometry was designed to ensure minimal pressure loss upstream from the entrance into the mold cavity,.and optimal shape for molding and demolding. For the hot embossing press, a vacuum chamber was designed containing the embossing sandwich, with the temperatures of the mold insert and of the substrate controlled through the press' heating/cooling system.

Experiments were performed to identify the important process parameters in injection molding of HARMs. It was established that mold insert temperature is of primary importance for the process, followed by melt flow rate. In hot embossing, it was argued that temperature of the polymer has most evident effects on the process, followed by variations in embossing force and embossing time. It was shown that the embossing time should preferably be long, to allow for relaxation of the macromolecular chains resulting in stress-free moldings.

Compared to HDPE, it was shown that PMMA is heat-sensitive, and that it requires special care including drying before dosage, and dosage under controlled temperature and shear conditions. When used in hot embossing, PMMA is advantageous compared with polycarbonate- PC, because it allows embossing at lower temperatures.

Three micro heat exchanger geometries were molded (and fabricated for testing), one stacked pattern and two cross flow patterns. Also, several DNA sequencing chips were microreplicated, using both injection molding and hot embossing. Also, a test pattern was designed for comparison between molding techniques. Molding was performed into two inserts of different heights (200 and 500 microns) using the same material (PMMA). An overall mean value of 1.25 % was reported for shrinkage of the plastic compared to the mold insert. Qualitative interpretation of the molding results showed differences in the demolding success rate between the two molding techniques combined with the two mold insert heights

CHAPTER 1. INTRODUCTION

The LIGA process involves three processing steps: X-ray LIthography, Galvanoformung (electroplating) and Abformung (molding) [1]. The LIGA process, as used at LSU, is based on bonding a sheet of poly(methyl-methacrylate) (PMMA) resist to an electrically conductive metal substrate, as shown in Figure 1.1. The resulting PMMA/metal substrate laminate is positioned behind an X-ray mask containing a pattern to be reproduced, and exposed to collimated radiation emitted from a synchrotron storage ring. During exposure, the molecular weight of the PMMA decreases in the irradiated areas due to bond breaking in the macromolecular chain. After the PMMA sheet is exposed, it is immersed in a developer and the irradiated areas are completely removed.

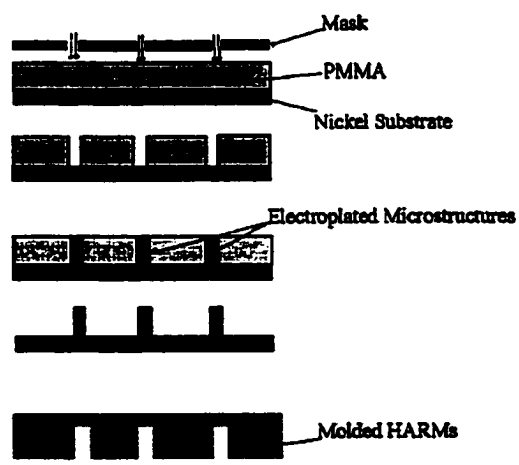

Figure 1.1 Schematic of LIGA

The resulting PMMA template is used to electroplate microstructures onto the substrate. After the electroplating process is completed, the remaining PMMA is stripped, resulting in a metal substrate covered with microstructures. The microstructure-covered substrate can represent the final product. Alternatively, it may

serve as a mold that can be inserted into a molding machine to repetitively produce secondary polymer or ceramic structures having the same geometry as the primary PMMA template. These molded structures represent an end-use object or can be used as a template for electroforming of new metallic objects. The commercial implementation of LIGA depends on the ability to rapidly generate inexpensive, mass-produced parts. Since the first two steps of this technique are inherently employing expensive and/or time consuming operations, the last step, molding, has to compensate for these expenses by mass producing low cost parts.

In the microreplication area, aspect ratio is defined as [2,3]:

$$Aspect\ Ratio = \frac{Maximum\ Height}{Minimum\ Lateral\ Dimension}$$

High aspect ratio microstructures, HARMs, have a height (or depth) measured in hundreds of micrometers and an aspect ratio of at least five. The present commercial molding processes, such as compact disk (CD) manufacture are limited to producing parts that have an aspect ratio on the order of 1 or less [4]. In addition, except for CDs, the available parts consist of small areas covered with microstructures [5, 6, 7]. Molding of large area plastic parts covered with HARMs is of particular interest for applications such as heat transfer, microfluidic elements, ceramics, etc. [8, 9].

A brief yet comprehensive review of the LIGA technique and its potential for microsystems was done by Bacher et al. in a paper dated in 1995 [2]. The authors of this paper are members of the German research team that first developed LIGA at KfK (Nuclear Research Center, Karlsruhe, Germany, and now Research Center Karlsruhe - FzK). Their earliest efforts date since the late 70's [10], thus they have the most

significant experience in the field. In this paper, Bacher and his coworkers present all the aspects of LIGA, including the modifications and extensions added to the technique.

Madou's review of LIGA [10] is also a comprehensive study. However, he bases his text on the experimental work and on the results of the same aforementioned German team, especially when presenting the molding step (also referred to as micromolding). Madou also briefly mentions the early efforts initiated at LSU in the field of molding, efforts that represent the beginning of the work hereby presented. From his knowledge, these are the first attempts to systematically approach the field of molding of LIGA microstructures in the United States. Harmening et al. [11] and Ruprecht et al. [1, 12] also part of the German team, give a condensed description of the molding techniques used in LIGA, briefly mentioning the principles of operation.

Referring to the work of the German research team at KfK, the representation in Figure 1.2 is an excerpt from Bacher's et al. paper showing a schematic classification of the molding methods used in LIGA. Classical molding methods were used, in principle, but several, sometimes severe, adaptations were made to fit the specific requirements presented by micromolding. The classical methods employed were reaction injection molding (RIM, figure 1.2 a), thermoplastic injection molding (figure 1.2 b) and compression molding (figure 1.2 c) also known as hot embossing. Independent of which method is used for molding, the final purpose is to produce a part that reproduces the geometrical shape and dimensions of the micropattern on the metallic mold insert. In order to achieve that, the material for molding has to completely fill up the microvoids on the insert, it then has to solidify sufficiently for separation (demolding), and it has to preserve its original geometrical definition over the period of usage.

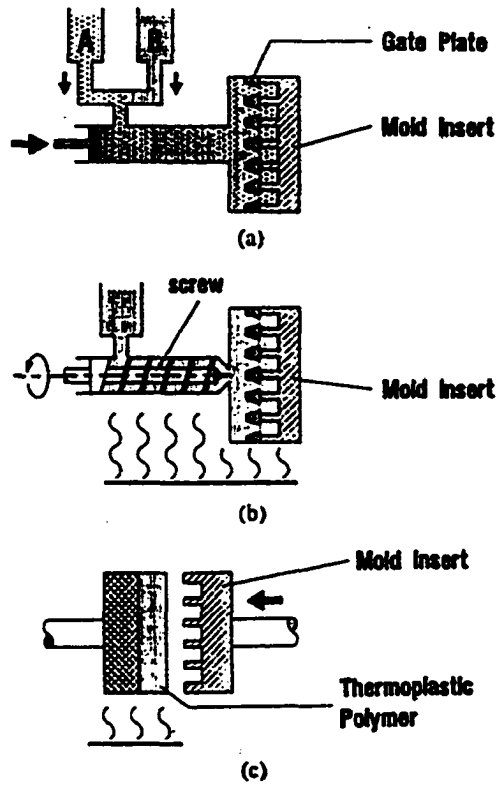

Figure 1.2 Classification of LIGA Molding Techniques:
a- RIM, b- Injection Molding, c- Hot Embossing [2]

These requirements are also applicable in the case of larger molded parts, but they become much more significant in the case of micromolding, since micromolding is performed on a small size scale on the order of micrometers. At this scale, the penetration into the narrow gaps is more difficult and the flow and thermal issues become more stringent. For instance, a high viscosity of the plastic melt or solution will make the filling step more difficult. Also, demolding can become a problem if the forces required to separate the plastic part from the metallic insert are on the same order as the structural strength of the microstructures.

Ehrfeld et al. [6] compiled a list of materials used in the LIGA process. A wide variety of thermoplastic polymers have been tried and applied for molding of LIGA microstructures, including polyoxymethylene, polystyrene, PMMA, polycarbonates, polyamides, and polyvinylidenefluoride. These polymers are suitable for specific applications, and the list of materials will continue to expand as new applications requiring new types of polymers are developed. The morphological structure of a certain polymer, its degree of crystallinity, the intermediate changes the polymer undergoes when changing phases, are all expected to affect the behavior of the polymer throughout the molding process and during the period of usage of the final product.

CHAPTER 2. INJECTION MOLDING

2.1 Injection Molding Techniques for Molding Microstructures

Injection molding for LIGA is currently employed as a primary technique for replicating micropatterns produced by X-ray exposure/electrodeposition processes [12]. The injection molding cycle starts by first melting and homogenizing the polymer inside the barrel of the injection machine, as shown in Figure 2.1. The polymer, in the form of pellets or flakes is loaded into a hopper. A screw, housed in a barrel, is used to shear, melt, and finally, pump polymer into the cylindrical zone located between the tip of the screw and the forward end of the barrel ("dosing"). When the desired amount of melt accumulates in front of the screw tip, the screw plunges forward and pushes the melt through the nozzle and the sprue and into the mold cavity where the mold insert for HARM replication is mounted. After the mold is cooled and the melt solidified, the two platens that form the mold are separated and the plastic part is ejected. Bacher et al. [2], Ruprecht et al. [12], and Ehrfeld et al. [6, 7] all mention the use of thermoplastic

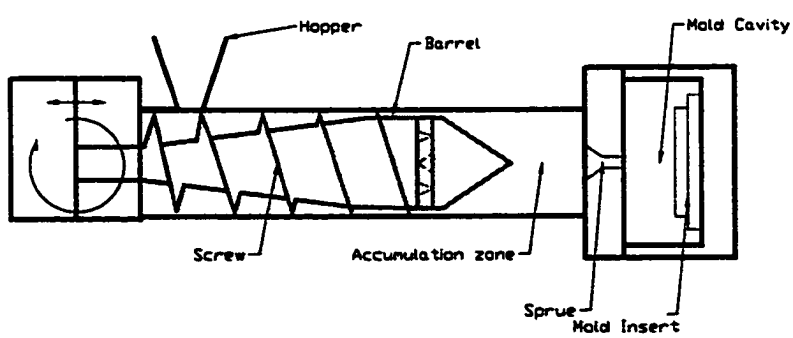

Figure 2.1 Schematic of an Injection Molding Machine

injection molding as one of the techniques for replicating LIGA microstructures. They mention the injection molding of compact disks (CD) as a method for molding microstructures. However, they also mention that the pits imprinted on the CD's surface have an aspect ratio of about one, which makes the technique unsuitable for direct application for molding HARMs. Ruprecht indicates, without going into any details, that a conventional injection molding machine as those used for CD fabrication can be used for molding of microstructures. The machine needs to be "expanded with special devices allowing the evacuation and temperature control of the tool for the complete filling of the mold"[12]. When describing this technique, the authors limit themselves to listing the main factors influencing the process, without showing actual values for any experimental parameters. The list of important parameters includes the tool temperature and the temperature of the melt, both of which have to be higher than in the conventional injection molding to prevent incomplete filling [7, 12]. They also indicate that "too high injection pressures or injection speeds lead to damages of the mold insert in an extreme case" [7]. Evacuation of the mold cavity is also mentioned as a critical factor for a successful injection [12].

2.1.1 Related injection molding applications

The small nature of the LIGA mold inserts makes the molding step more challenging than the classical injection molding processes. However, some industrial applications of injection molding of macroscopic objects can be compared to injection molding of HARMs, because similar fundamental flow and heat transfer principles govern the process both at macro and at micro scale. For instance, molding of thin wall parts also involves filling of mold patterns having high aspect ratios. As the thickness of

the wall is decreased, incomplete filling (short shot) can become a problem due to premature solidification of the melt. Typical applications of thin wall parts include cellular phone components, laptop and notebook computer components, disposable containers and cups, medical equipment components, etc [4]. Fasset [4] indicates that increasing the injection speed coupled with using a smaller injection machine leads to a more efficient and safe production of such thin wall molded parts. In order to achieve complete filling of a high aspect ratio mold, the polymer melt has to be as fluid as possible, therefore its viscosity must be kept minimal. To decrease the viscosity, the polymer melt is heated to higher temperatures, thus increasing the potential for thermal degradation. Using increased injection speeds rather than elevated temperatures results in a decrease of the degree of degradation of the polymer. This is due to the shear thinning character of the polymer that leads to a lower viscosity without thermal degradation of the polymer. Fasset reports that an increase of the injection speed from 10 cm/sec to 36 cm/sec led to a decrease by a factor of about 3.3 in polymer degradation as measured by percent decrease in melt viscosity. Also beneficial was the selection of an injection machine with a smaller barrel, because a shorter residence time was imposed to the polymer melt, thus less time for the thermal degradation to occur. The melt viscosity of the degraded polymer decreased 300% as compared to that of a polymer that was used in a barrel four times smaller.

Breuer takes the comparison between CD manufacture and microinjection molding one step further and shows that producing free standing miniature parts is more challenging than molding CD storage media because the overall size of a CD is much larger than that of a LIGA part [13]. In the case of micromolding individual parts, the

runner system dwarfs the actual microparts, leading to a complicated design and an uneconomical production. He proposes a few modifications of the classical plasticizing unit such as eliminating or reducing the runner system, or the introduction of open hot-runner systems such that the molded part can be reached without a runner. Moreover, he suggests that given the very small shot weight (on the order of a few grams or less) a reciprocating plasticizing screw is not suitable anymore. A reduction of the plasticizing unit cannot be done past a certain limit dimension of the screw diameter because of the increased probability of a break and because the positive plasticizing characteristics are reduced with a low screw stroke. Breuer presents an alternative to using a machine with reciprocating screw plastication by using an injection unit where the melt is prepared into a separate plastication unit, and then sent into an injection unit used to fill the mold. Such a machine is now commercially available, being produced by Battenfeld Kunstatoffmachinen [14]. The machine offers the advantage of a more accurate control of the shot size and a more efficient usage of the material to be injected (a ratio of 60/40 part/sprue+runners as opposed to 34/66 for older systems). Cycle times are also reduced by minimizing cooling time and handling time.

Summarizing the information with respect to thermoplastic injection molding, it can be concluded that the most important process parameters are melt and mold temperatures, coupled with the injection pressure/ injection speed. The experience gathered from related molding processes indicates that selection of the injection machine, combined with a proper design of the mold (runner-gate system and cavity) and evacuation of the mold prior to injection are essential for a successful injection molding of HARMs, as those produced by LIGA.

2.2 Injection Molding Equipment

The μSET group at LSU is currently developing injection molding methods for producing large area plastic parts covered with HARMs. The work has been centered on using a standard injection molding machine for a nonstandard application such as micromolding. Immediately, one should notice that the equipment costs are much lower if a standard, commercially available molding machine is used for micromolding instead of a complicated, non-standard application-specific machine. The injection machine, type Arburg Allrounder® 170 CMD 150-45 [15], is designed with a reciprocating screw that both melts and injects the polymer into the mold cavity. The reciprocating screw is capable of two types of motion: it can rotate around the longitudinal axis of the barrel and it can translate along the same axis. Inside the barrel, the material is melted by thermal input from the electrical heating jackets (bands) and by the shearing action of the rotating screw. As stated above, the work done throughout this study was based on using a commercially available, general-purpose injection molding machine. Thus, given the differences between a classical injection molding process and the more special process of micromolding, a few adaptations had to be made to the equipment, none of which was cost-intensive.

First, a new mold, composed of two halves, was designed to hold the micro-mold insert. The two mold halves were designed such that, when closed together they form a cavity inside which the insert is placed and where the plastic melt is injected to fill the micro-pattern onto the insert. The mold design was based on what was expected to be specific requirements related to pushing the plastic melt into the high aspect ratio microstructures. Because a high pressure drop was expected to occur within the

microgaps on the mold insert, a runner/gate system was completely eliminated from the mold design. This allowed for a direct access of the melt with minimal pressure loss upstream from the mold cavity. The design resulted in a single cavity mold; given the experimental nature of this work, together with the small capacity of the injection machine, the purpose was not to design a multi-nested mold but one that could hold a single mold insert. Knowing that complete filling of the microvoids will be influenced by the temperature of the insert, the design included a heating/cooling system. The system was mounted onto the mold platen holding the mold insert. The heating system consists of four heating cartridges (rods) mounted in channels running vertically into the mold platen. Heating the mold is controlled from a temperature controller mounted on the control panel of the injection machine and coupled with a thermocouple that senses the mold platen temperature. The cooling system consists of three channels interplaced between the heating elements. The heating/cooling channels were uniformly distributed to cover the mold insert area of the mold cavity. The channels were drilled such that a better uniformity of the temperature can be achieved.

Aluminum was used as the material for the mold platens because it provides several advantages over the more classical solution using stainless steel. First, aluminum is strong enough to resist the relatively small loads imposed by the clamping system to the mold, given the relative small shot size. Also, aluminum has the advantage of being easier to machine. Second, aluminum offers the advantage of a lower thermal inertia than stainless steel. This is advantageous because the mold has to be heated at the beginning of the cycle in order to prevent premature freezing of the melt; it then has to be cooled down to the demolding temperature for the part to be

ejected, and the low thermal inertia of aluminum shortens the portion of cycle time dedicated to heating/cooling the mold.

Another requirement for micromolding, in addition to controlling the barrel temperature, the injection rate, and the mold temperature, is to vent the micromold prior to injection [12]. At macroscale, air entrapment inside molds is usually avoided by venting the air through very fine slits. These slits are machined on the interior surfaces of the two mold platens, in the parting line, and the air is expelled as the melt fills the mold. In other cases, the clearance gaps around the ejector pins provide sufficient volume to vent the mold, without the need for venting slits. In micromolding, a complicated fluid front may lead to air entrapment if air is present inside the mold prior to injection, i.e. if the mold cavity is not under vacuum before injection begins. Thus, the injection machine has to be fitted with a vacuum system for venting the mold prior to injection. A rotary vane vacuum pump was connected to the mold through a vacuum port machined into the stationary mold plate. To prevent plastic melt from being sucked into the vacuum line upon injection, the vacuum port is interfaced with the mold cavity through a pill of sintered metal (stainless steel). The pill is held in place with a hex cap screw whose core was drilled out along its longitudinal axis. A schematic drawing of the setup is shown in figure 2.2.

Additional equipment was necessary for the heating/cooling system and for the vacuum system. Thus, a general-purpose water pump was connected with the cooling channels and a 25-gallon water tank was built to economically fit inside the space available in the injection machine's chassis. The water flow could be controlled with a ball valve, and the temperature could be lowered by adding ice to the water.

Figure 2.2 Schematic Drawing of Vacuum Port

The vacuum was achieved using a laboratory size pump capable of evacuating the mold cavity down to 50 mmHg in less than 1 second. A photograph of the mold halves is shown in the next sub-chapter, together with mold design solutions chosen to fit the specific requirements of the injection molding material.

2.2.1 Characterization of Molding Materials

- **Differential Scanning Calorimetry (DSC)**

DSC was used to determine the softening region for the thermoplastic polymer used in our molding experiments, namely high density polyethylene, HDPE. This calorimetric technique, described in detail elsewhere [16] is based on the fact that a transition such as crystallization or vitrification is associated with a change in thermal properties of the sample under study. This change can be identified when comparing the sample with a reference. By monitoring the temperature difference between the sample and the reference, or by measuring the energy input necessary to maintain both the sample and the reference at the same temperature, one can determine the location where the transition occurs and also the type and magnitude of this transition. DSC analysis

preformed on HDPE 25, seen in figure 2.3, yielded a softening interval between 120 and 140 °C, with the peak at 132.5°C. The peak is considered the melting temperature, and it was taken as a reference in determining the rheological parameters of HDPE 25.

- **Capillary Rheometry**

Polymeric melts are dual in nature: they exhibit both a viscous character and an elastic character. The visco-elasticity is always present in the response of the polymer fluid to an imposed stress or deformation. One way to control the injection molding process is to impose a certain flow rate at which the melt is injected, thus imposing a stimulus in the form of shear rate (rate of deformation). The magnitude of the resulting shear stress

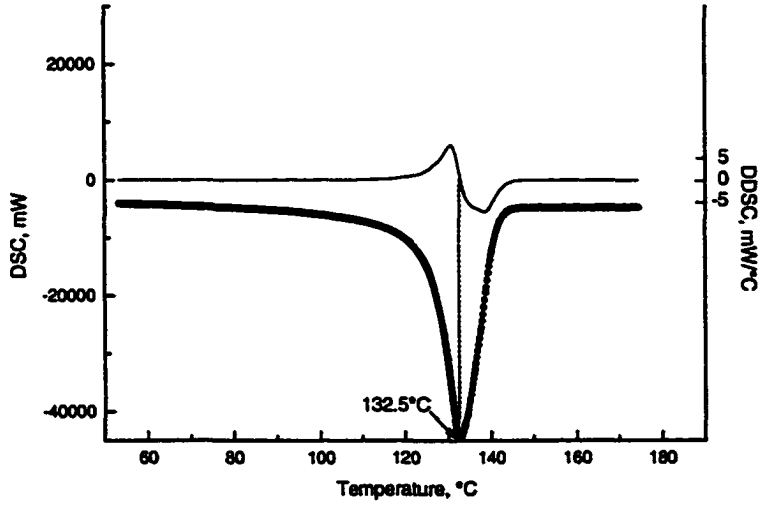

Figure 2.3 DSC and DDSC curves for HDPE 25

is related to the imposed signal through the constitutive equation characteristic to the polymer melt used. For polymer melts, one of the most widely used constitutive equations is the Power Law model, proposed by Ostwald and de Waele. This model relates the shear stress to the shear rate by:

$$\tau = m \cdot (\dot{\gamma})^n \qquad (1)$$

where τ (Pa) is the shear stress, $\dot{\gamma}$(sec^{-1}) is the shear rate, m ($Pa \cdot s^n$) is the consistency and n (dimensionless) is the flow index. For $n = 1$ the Ostwald de Waele model reduces to Newton's law of viscosity with m being the viscosity. If an apparent viscosity is defined as the local value corresponding to a Newtonian behavior

$$\tau = \eta_a \cdot \dot{\gamma} \qquad (2)$$

then the Power Law equation can be written as:

$$\eta_a = m \cdot (\dot{\gamma})^{n-1} \qquad (3)$$

It is important to note that the consistency m is strongly dependent on temperature, following an Aarhenius-type relationship:

$$m = m_0 \exp[-a(T - T_0)] \quad (4)$$

The determination of the pre-exponential factor m_0 and of the exponent a can be done using capillary rheometry. The technique, involving the forced flow of a polymer melt through a capillary die is described in detail elsewhere [16]. For the molding material of choice, DOW high density polyethylene with Melt Index 25, the determination of the Ostwald deWaele parameters was performed at three different temperatures (190, 210, and 230 °C), corresponding to the processing temperatures inside the injection molding machine. The results of these determinations are summarized in Figure 2.4. The plot shows an exponential decay of the apparent viscosity as a function of shear rate. From the fitting parameters of the data plotted in figure 2.4, it can be noted that the value of consistency m (pre-exponential factor) varies with temperature, while the value of the flow index n (exponent) can be considered constant over the temperature range.

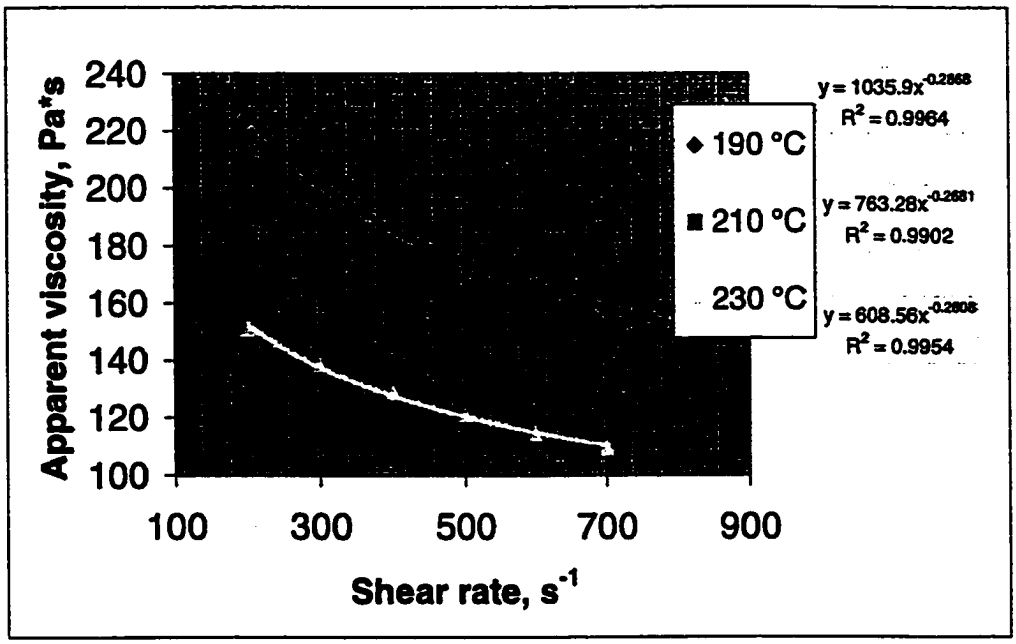

Figure 2.4 Apparent Viscosity vs. Shear rate at 190 °C, 210 °C, and 230 °C

The temperature dependency of m is shown in the plot in Figure 2.5. The data plotted in this figure represents the values of m at three different temperatures, as determined by curve-fitting the data in figure 2.4. The Aarhenius-type fit in figure 2.5 yields:

$$m = 2196.3 \cdot \exp[-0.0133(T - T_0)] \quad (5)$$

where T_0 is the melting temperature of the polyethylene used in the injection molding experiments. The determination of the value of T_0 by DSC was shown previously. The thermal analysis determined the T_0 value of 132.5°C.

2.3 Injection Molding Experiments

The experimental work has been oriented in two main directions: first, experiments were performed to investigate the influence of injection speed and mold temperature as two main parameters for the process. Second, the replication of various mold inserts was done using mold inserts with aspect ratios as high as 11:1, and minimum lateral dimension as small as 20 μm.

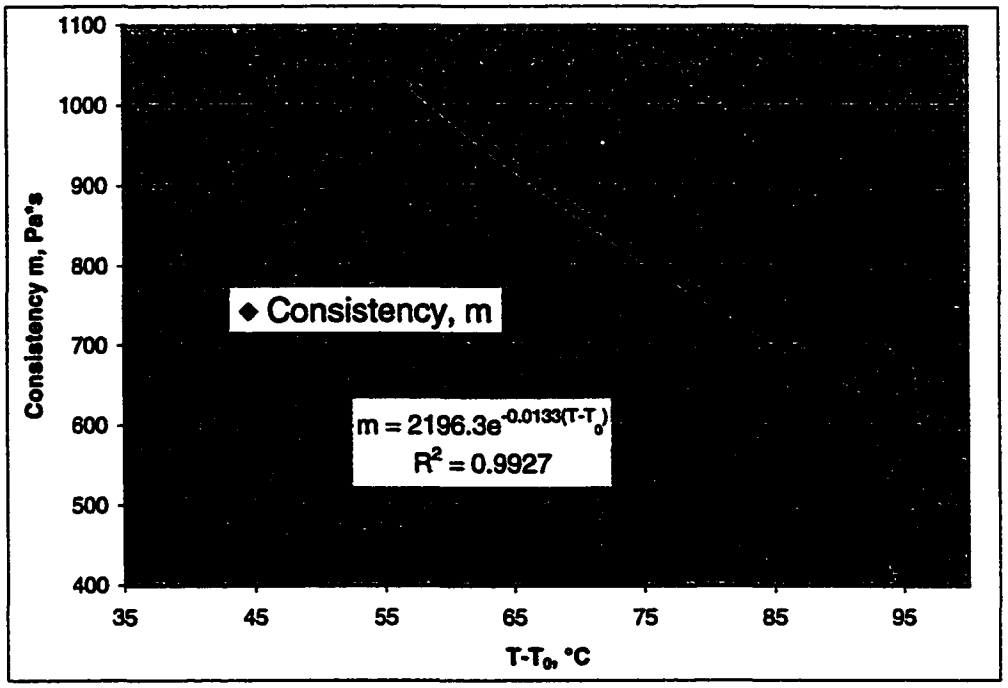

Figure 2.5 Preexponential Factor and Exponent from *m* vs. *T-To*

Regarding the first research goal, six series of plastic injection experiments were performed using the laboratory-scale injection molding machine Arburg Allrounder 170 CMD 150-45. Throughout the experiments, the temperature field across the barrel was kept identical. In the first series of experiments, the temperature of the mold cavity at the beginning of the injection cycle was equal to room temperature, while the injection speed, expressed as melt flow rate, was varied from 10 to 80 cm^3/s. In the five subsequent series, the mold temperature was set at 60 °C, 80 °C, 100 °C, 120 °C, and 140 °C while the injection speed was varied as in the first series. The demolding temperature was set at 50 °C. The evolution of the temperature of the mold during the cycle time was continuously monitored with a thermocouple mounted in the movable platen.

The mold insert is shown in Figure 2.6. The posts are made of nickel with square cross-section, 180 μm x180 μm, and are approximately 750 μm high. The gap between two adjacent posts is 90 μm. The results of the six series of experiments are

Figure 2.6 Insert Used for Molding: posts are 180x180 μm, 600 μm tall

given in Table 2.1. In each experiment, the distance the polymer penetrated into the space between the microposts was measured and reported as percent volume filled. This value was subtracted from 100%, the result representing the percentage of the microgap volume remaining unfilled at the end of the injection cycle. Scanning electron microscope (SEM) micrographs showing molding results from flow rate extremes (10 cm^3/s, and 80cm^3/s) are provided. Figures 2.7a and 2.7b show micrographs of part of a homogeneous field (2.5-cm diameter) of HARM HDPE microstructures produced by micromolding when the mold cavity was preheated to 140°C. The micrographs show complete penetration into the mold insert, with well-defined plastic features that accurately reproduce the mold geometry. A quantitative study of the accuracy of the reproduction is given in sub-chapter 2.5. It is also important to note that all the curvatures and the non- rectangular features on the micrographs are a result of the

Table 2.1 Results of Molding Experiments.

% unfilled	Mold temperature, °C					
		20	60	80	100	120	140
Flow rate, cm^3/s	10	4.99	4.59	3.84	4.90	0.48	0.00
	20	15.03	10.16	6.57	2.74	0.00	0.00
	30	16.57	9.07	6.11	2.89	0.00	0.00
	40	15.35	6.98	4.66	2.85	1.73	0.00
	50	13.54	5.29	3.49	2.63	0.00	0.00
	60	9.92	5.03	2.42	2.45	0.00	0.00
	70	7.64	4.47	2.12	2.97	0.00	0.00
	80	3.35	5.04	1.87	1.87	0.00	0.00

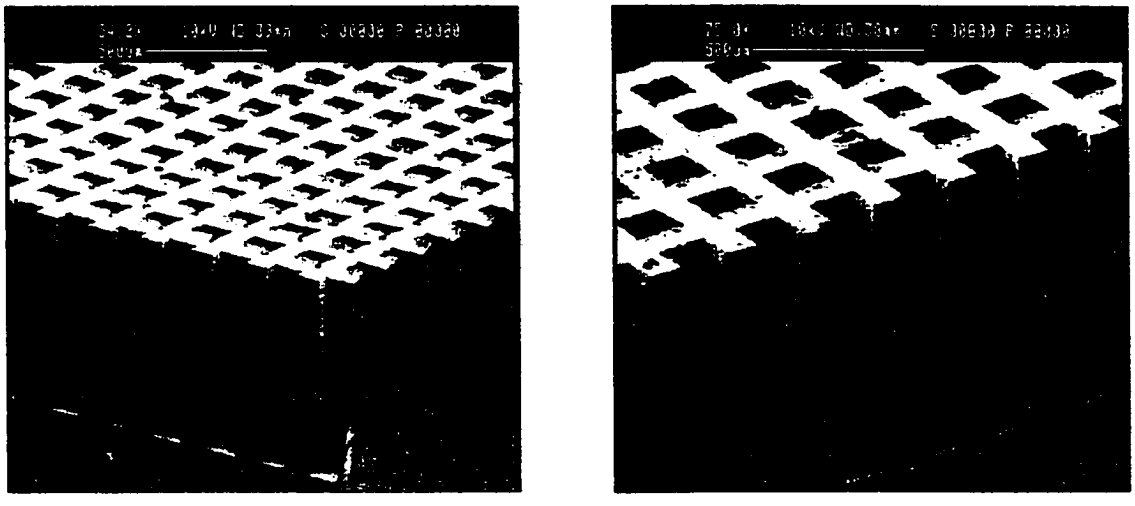

a **b**

Figure 2.7 HDPE molded part, mold at 140 °C, **a:** melt flow rate = 10 cm^3/s; **b:** melt flow rate = 80 cm^3/s

way the sample was prepared, i.e. simply by sectioning with a double-edge razor blade, and are not a manifestation of the molding process. Figure 2.8 shows a larger area of the part shown in Figure 2.7.

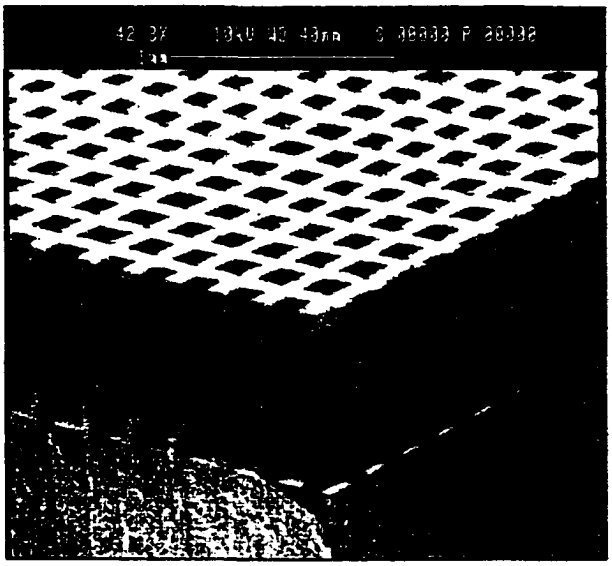

Figure 2.8 General view of HDPE molded part

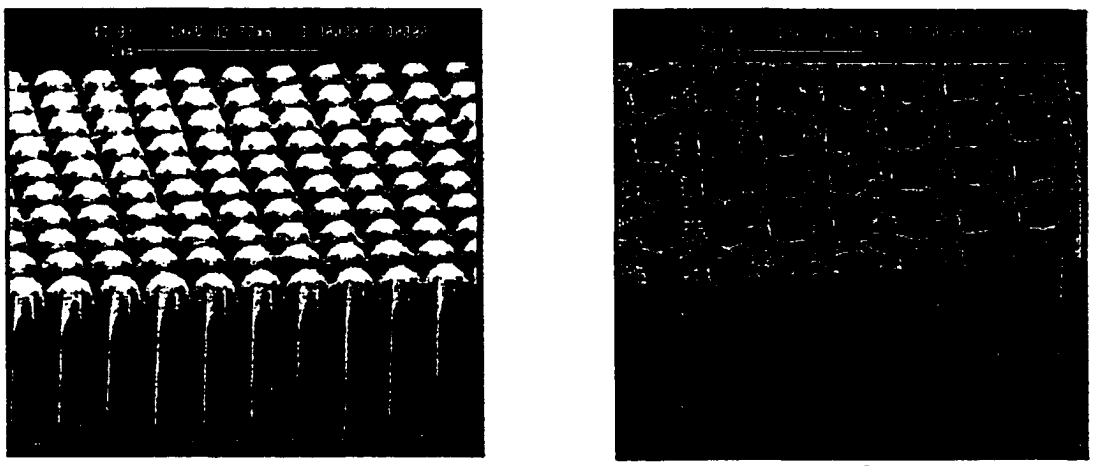

a **b**

Figure 2.9. HDPE molded part, mold at room temperature, **a:** melt flow rate = 10 cm^3/s; **b:** melt flow rate = 80 cm^3/s

Figures 2.9a and 2.9b show examples of molding experiments when the mold cavity was at 20 °C, but at two different injection rates (10 cm^3/s and 80 cm^3/s). In both cases, the polymer did not completely fill the mold cavity, although higher injection rates did reduce the magnitude of the problem. The premature freezing of the melt, also called "cold finger effect" is evident, explaining the "bumpy" appearance of the sample injected at 10 cm^3/s and the presence of weld lines on the sample injected at

80 cm^3/s. The melt penetrates deeper at the intersection of the perpendicular microchannels where the ratio of contact area/volume is the smallest, producing a lower rate of heat transfer and a longer time before which freezing occurs. The "mountain-valley" pattern is thus produced with the mountains occurring at the corners of four posts. Figure 2.10 presents graphically the information tabulated in Table 2.1, plotting the percent volume unfilled as a function of injection speed at different mold temperatures. In figure 2.10, it can be seen that, at lower temperatures of the mold,

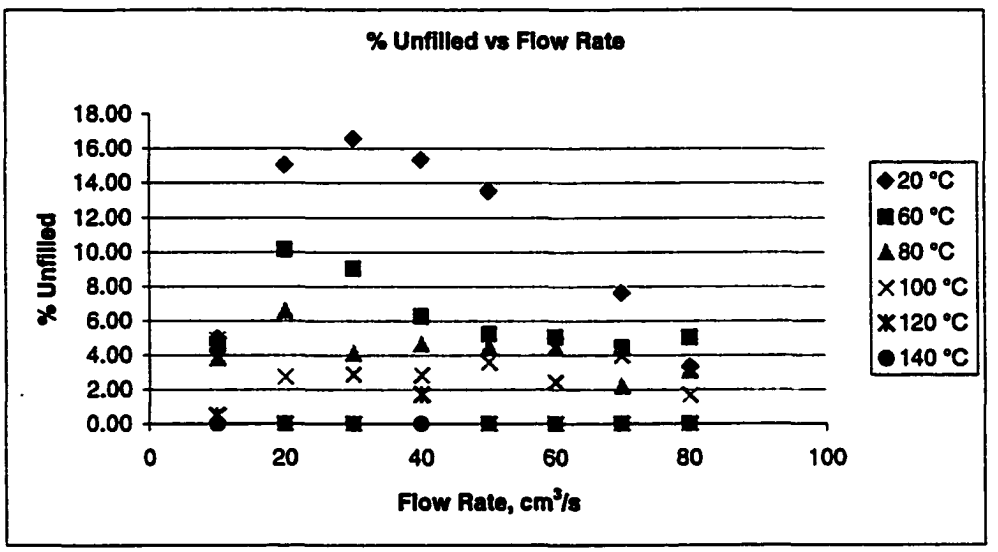

Figure 2.10. Plot of percent unfilled as function of melt flow rate

increasing the injection speed enhances the filling of the mold cavity. At high mold temperatures, the injection speed becomes less important. At 140 °C (above the melting point of HDPE), the cavity is completely filled over the entire range of injection speeds.

Figure 2.11 shows a comparison between the composition of the injection cycle time for the cases where the mold was heated at 140 °C and where the mold is unheated. In addition, a literature value is given for reference. The large difference between the values of the overall cycle time is due to time needed to thermally cycle the mold in the

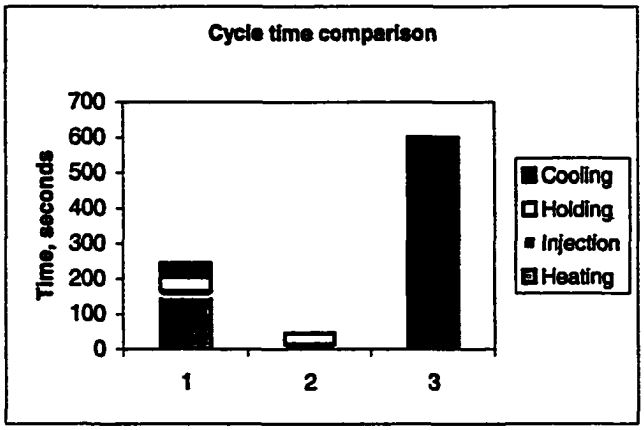

Figure 2.11 Comparison of duration and composition of cycle times between injection cycles done at two mold temperatures: 1- 140°C; 2- 20°C; 3-overall literature value [12]

case where the mold is heated. However, even at the higher values, the overall cycle time is still shorter than the overall values reported in the literature [12].

2.4 Results and Discussion

A simplified model can be used to qualitatively predict the results given in Table 2.1 and in Figure 2.10. When the polymer is first injected into the mold cavity, the assumption is made that the spaces in the mold cavity not associated with the voids between the microstructures (microvoids) are filled up first. This assumption is based on the fact that flow resistance into these spaces is negligible compared to the resistance between the microstructures. Once these spaces are filled, the polymer melt begins to penetrate into the microvoids in the insert. The time for these spaces to be filled is approximately the volume of the microvoids (cm^3) divided by the injection rate (cm^3/sec). For the insert shown in Figure 2.6, the time required to fill the microvoids ranges from $t = 0.002$ sec ($Q = 80\ cm^3/sec$) to $t = 0.016$ sec ($Q = 10\ cm^3/sec$).As the polymer penetrates the microvoids, heat transfer occurs between the melt and the insert. The thermal boundary layer thickness in the melt, δ_t, is approximated by the expression:

$$\delta_t = \sqrt{\pi \alpha t} \quad (6)$$

where the thermal diffusivity, α, is approximately 0.3×10^{-6} cm^2/s. For values of the time t= 0.002 and 0.016 seconds, δ_t equals 43 micrometers and 122 micrometers, respectively. Since the width of the channel between parallel posts is approximately 90 micrometers, the thermal boundary layers growing from parallel post surfaces meet, even at the fastest flow rate. Qualitatively, this means that the melt temperature is dramatically reduced during the time required to penetrate the microvoids. A simple model has been developed to predict whether the polymer will quench and solidify before it completely fills the mold cavity. The model is based on the following assumptions:

- The two main components of the total pressure drop between the barrel and the melt front inside the microchannels are: i) the pressure drop across the sprue and , ii) the pressure drop across the microchannels. Therefore,

$$\Delta P_{total} = \Delta P_{sprue} + \Delta P_{\mu channel} \quad (7)$$

- Due to the existence of a vacuum inside the mold cavity, the pressure at the melt front can be approximated to zero;
- As the injection pressure reaches the value 1300 bar, the injection stops. This value represents the maximum pressure output deliverable by the hydraulic system;
- The flow through the sprue can be approximated as fully developed flow through a cylindrical channel;
- The flow through the microchannels (between adjacent microposts) can be approximated as unidirectional flow between parallel plates, in a direction perpendicular to the substrate on which the posts are supported;

- The polymer melt has a non-Newtonian, shear thinning nature that can be described by the Ostwald-de Waele model. The melt index n is assumed constant, while the consistency m is a function of temperature given by:

$$m = m_0 \exp[-a(T - T_0)] \qquad (8)$$

where m_0, a, and T_0 are constants specific to the HDPE used;

- Viscous dissipation due to shearing of the melt along the sprue determines the mean temperature of the melt at the exit from the sprue;
- Heat transfer between the melt and the insert is approximated as follows:
    - the insert temperature is constant
    - the velocity profile of the melt within the insert is uniform.
    - heat transfer within the polymer is one dimensional (normal to the surface of the microstructures)
    - the mean temperature of the melt within the microchannel is equal to the mean temperature of the melt at the melt-vacuum interface.
    - the temperature of the microposts remains constant during injection.
    - the temperature profile across the polymer at the melt front is calculated using analytic formulas for a plane wall with convection, Biot = ∞.

The model calculates the total pressure drop required for complete penetration into the microchannels. Based on these assumptions, the following set of equations was used.

For calculating the pressure drop across the sprue:

$$\Delta P_{sprue} = P_{injection} - P_{sprue-exit} = \left[2m_1 \cdot \left(\frac{3n+1}{\pi \cdot n} \right)^n \right] \cdot \frac{L_{sprue}}{R_{sprue}} \cdot Q^n \qquad (9)$$

$$m_1 = m_0 \exp[-a \cdot (T_{sprue} - T_0)] \qquad (10)$$

$$T_{sprue} = T_{melt} + \left(\frac{2^{3+2n}}{\pi^n} \cdot \frac{m_1}{3+n} \right) \cdot \frac{L_{sprue}}{R_{sprue}} \cdot \frac{Q^n}{\rho \cdot c_p} \qquad (11)$$

Equation 9 shows that ΔP_{sprue} is a function of two variables, Q and m_1. From Equation 11, as Q increases, the value of T_{sprue} increases and (from Equation 10) the value of m_1 decreases. Therefore it is impossible to know whether ΔP_{sprue} increases monotonically with Q without knowing the specifics of the problem (geometry of the sprue, flow rate and material properties).

For calculating the pressure drop across the microchannels:

$$\Delta P_{\mu channel} = P_{top} - P_{front} = \left[m_2 \cdot \left(2^{n+1} \cdot \frac{2n+1}{n} \right)^n \right] \cdot \frac{L_{\mu channel}}{W^n \cdot H^{2n+1}} \cdot Q^n \quad (12)$$

$$m_2 = m_0 \exp[-a(T_{\mu channel} - T_0)] \quad (13)$$

$$T_{\mu channel} = T_{sprue} + \\ + (T_{insert} - T_{sprue}) \cdot \left[1 - 0.807 \exp\left(-2.46 \cdot \alpha \frac{Area \cdot L_{\mu channel}}{Q \cdot W^2} \right) \right] \quad (14)$$

where W is the total width of the parallel-plate flow, H is the half-width between two adjacent posts, *Area* is the area on the insert open to the flow. The same analysis can be made here as in the case of the sprue: the evolution of $\Delta P_{\mu channel}$ as a function of flow rate Q cannot be predicted only from Equation 12. Rather, $T_{\mu channel}$ has to be calculated first and a value of m_2 has to be determined before evaluating $\Delta P_{\mu channel}$.

The simplified model was used to predict the total pressure drop required to completely penetrate to the bottom of a mold insert covered with posts 750 microns tall, with the gap between posts of 90 microns. The same combination of values for mold

temperature and melt flow rate was used, as in the experimental part of our study. The results plotted in Figure 2.12 indicate that, as the temperature of the mold increases, less pressure is necessary to completely penetrate into the 750 microns deep gaps.

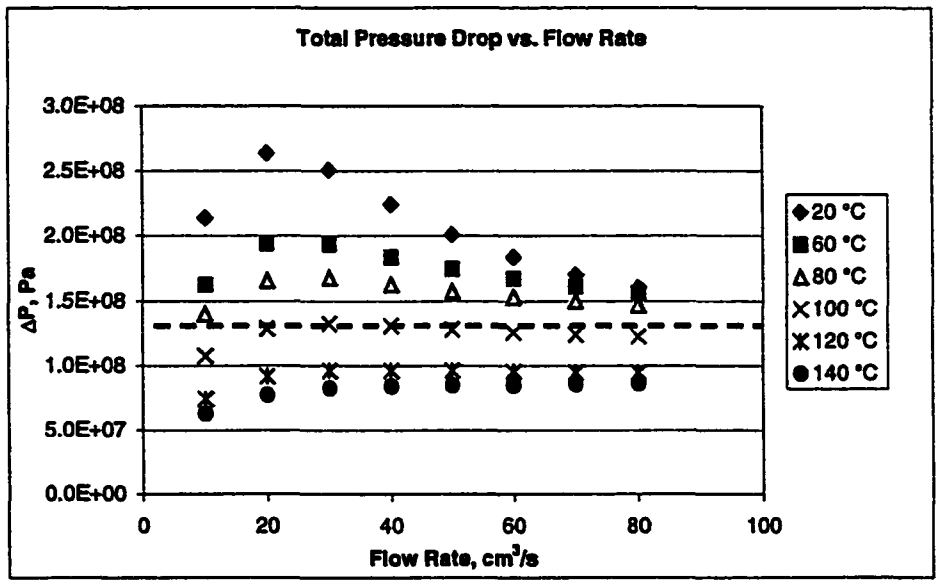

Figure 2.12 Predicted total pressure drop vs. flow rate, at different mold temperatures

The model predicts that combinations of mold temperature and melt flow rate resulting in data points located above the 1300 bar line will correspond to incomplete penetration of the plastic into the mold insert. This is due to the assumption that the flow stops when the total pressure drop exceeds 1300 bar. Inversely, points located below the 1300 bar line represent combinations of parameters that lead to complete penetration into the mold insert. In summary, the model predicts that heating the mold at temperatures above 100 °C leads to injection molding of high-quality polymer HARMs at all flow rates, while temperatures of the mold below 100 °C do not ensure complete penetration into the mold insert, independent of the flow rate. These predictions are in qualitative accordance with the experimental results given in Figure 2.10: in our experiments we found that injection cycles conducted at mold temperatures

higher than 120 °C lead to complete penetration into the mold insert independent of the melt flow rate. Below 120 °C, although a high injection speed improved the process, penetration of the mold insert was incomplete in all cases. The experimental values of 120°C and 140 °C have a physical meaning related to the polymer used in our experiments. A temperature of 120 °C corresponds to the onset of the melting process for the HDPE used, as determined by DSC measurements. Also determined by DSC, a temperature of 140 °C represents the upper limit of the melting interval (as mentioned before, the melting interval is centered on 132.5 °C). Qualitatively, the model predicts the experimental results shown. However, the model gives 100 °C as the lower value of the mold temperature at which injection is successful as opposed to the experimental value of 120 °C. Given the simplifying assumptions for the model, such differences between model and experiments are expected.

2.5 Examples of Injection Molding Results

2.5.1 Injection-molded Parts

The second avenue that has been pursued is molding plastic HARMs that accurately reproduce the pattern on the mold insert. The challenge consisted in molding large area HARMs covered with microstructures having aspect ratios of 10:1 or above. An example is a pattern composed of rectangular posts 1000μm tall and 180μm on the side, with the gap between posts of 90 μm. A micrograph of the molded part is shown in Figure 2.13. The injection was carried out at 140 °C and with an injection rate of 70 cm^3/s. After mold-filling, the mold was cooled down to the same demolding temperature as in the case of the 600 μm insert (50°C). Similarly to that previous case, the demolding was achieved easily, preserving the structural integrity of the plastic part

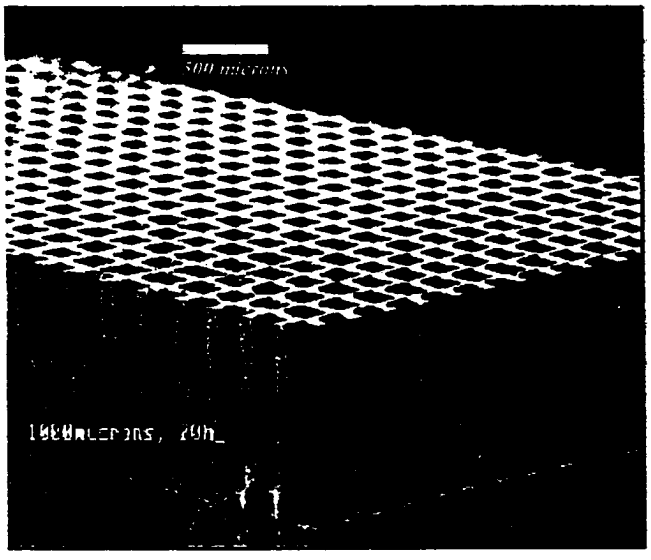

Figure 2.13 Micrograph of HDPE HARMs: Aspect Ratio 11:1

Another example of a successful molding experiment is that of a "lab-on-a-chip"-type pattern, composed of small reservoirs interlinked by microchannels. A portion of the pattern on the mold insert is shown in Figure 2.14. The material for molding was HDPE, MI 25. The smallest lateral dimension on the pattern is 80 microns, with a height of 500 microns. The challenge in molding this pattern consisted in replicating the narrow, rather fragile microloops. The injection molding cycle was carried at a mold temperature of 130 °C and an injection speed of 30 cm^3/s.

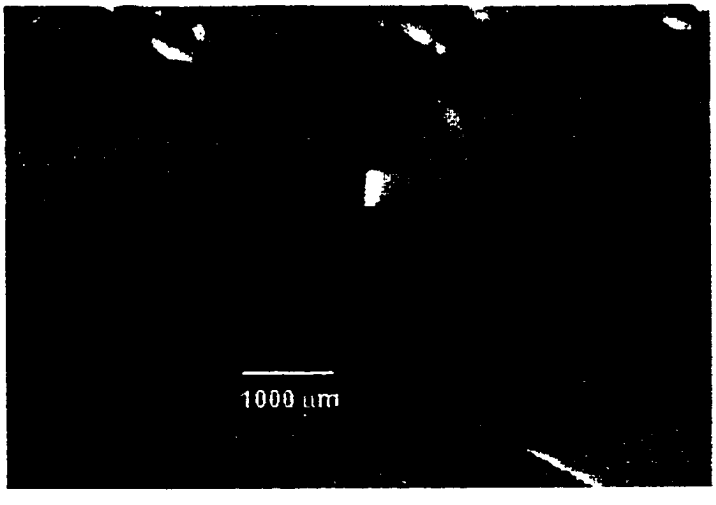

Figure 2.14 Lab-on-a-chip Mold Insert

The injection speed was lower than in the previous example, because of the fine walls on the mold insert. Lowering the injection speed reduced the probability that the advancing melt front would damage the fine structures on the insert. SEM micrographs of the molded structure are shown in Figure 2.15 a and b. Figure 2.15a shows proper replication of the meandering microchannel, the piece missing from that area corresponds to an imperfection that existed on the mold insert.

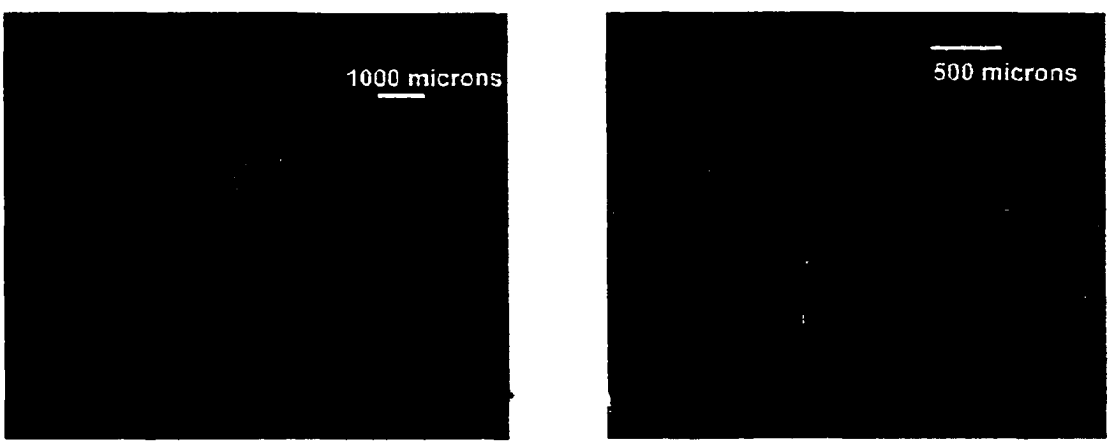

Figure 2.15 Molded Lab-on-a-chip pattern: a- general view; b- close-up

Figure 2.15b is a close-up of the lower right area in Figure 2.15a. The image shows that the top and bottom surfaces of the molded part have different roughness. This is an indication of the ability of the molding step to intimately reproduce even the finest geometrical characteristics existent on the mold insert. One can say that, after optimizing the molding process, the molded part will be as good as the mold insert.

2.5.2 Injection Molding of Polymethylmethacrylate (PMMA)

PMMA is a material widely used for its optical properties. It has excellent transparency (optical absorption at 514.5 nm is 0.084 dB/m), it has a refractive index of 1.49 and the Abbe number is 58. Because of these properties, PMMA is often used as glass replacement, thus its trade name "plexiglas". For example, one area in which

PMMA is increasingly used to replace glass is in microfluidic elements. Such systems, for instance DNA sequencing microsystems have at their core a flow element consisting of a long and narrow microchannel, used to separate macromolecular segments of different lengths based on differential flow. The microchannel on such a "chip", as developed in the Chemistry Department at LSU, has typical dimensions of tens of millimeters length, tens of microns depth, and tens of microns width, with vertical aspect ratios up to 8:1. Bioseparation systems are traditionally made of glass, but making DNA sequencing chips using PMMA offers a series of advantages over glass. First, PMMA chips can be mass-produced by molding and can be made available as relatively inexpensive disposable parts. Secondly, as for glass, the surface chemistry of PMMA can be modified to enhance chemical compatibility, and work to improve the properties of PMMA by means of chemical modifications of the surface is currently carried out. This, coupled with the fact that PMMA can be shaped by any of the thermoforming methods used for thermoplastic polymers makes it a good choice for biomedical applications. Also advantageous for PMMA is its machineability.

Research work was carried out to accurately replicate the DNA sequencing microchannel patterns developed by the μSET group. It was found that, when injection molding PMMA, several precautions have to be taken for the molded part to have optimal characteristics. A description of these requirements is later summarized in Table 2.2. PMMA is a temperature-sensitive material, which easily decomposes into monomer above 300 °C. The decomposition mechanism consists of fast "un-zipping" of the long macromolecular chain into short monomer molecules. By comparison, HDPE starts to decompose at 300 °C, too, but the decomposition occurs at a much slower rate,

through random breakage of the chain. Figures 2.16 a and b show thermogravimetric data for PMMA and HDPE. It can be seen that the onset of the degradation is at around 300 °C for both materials, but the degradation rate is much slower for HDPE compared with PMMA. At 350 °C, the original solid PMMA sample has lost 95.6% of its mass as gaseous monomer, compared to a loss of just 0.17% for HDPE. The experimental data presented in figures 2.16 a and b indicates that exposing PMMA at temperatures above 300 °C results in degradation of the macromolecular chain as gaseous monomer. Moreover, the degradation is occurring much faster in PMMA compared with HDPE, and this also holds true inside the injection molding machine. It was discussed that to ensure minimum viscosity for the melt to completely penetrate into the microstructures, the barrel of the injection molding machine is kept as hot as possible without degrading the polymer.

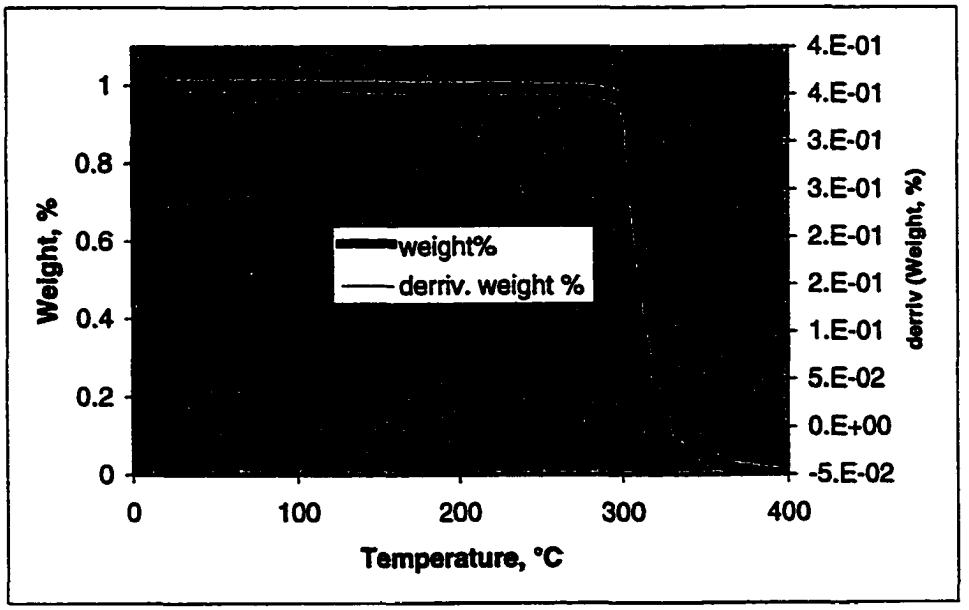

Figure 2.16 a TGA Analysis for PMMA

The back-pressure does not allow the outgassing of the monomer from the melt pool dosed for injection. Applying a higher holding pressure after injection prevents

shrinkage and also prevents the escape of the monomer from the part. It is assumed that the decomposition is slowed down under pressure, minimizing unzipping. However, too high a holding pressure leads to overpacking, thus it leads to a stressed part and difficulties in extracting the cooled-down part from the mold.

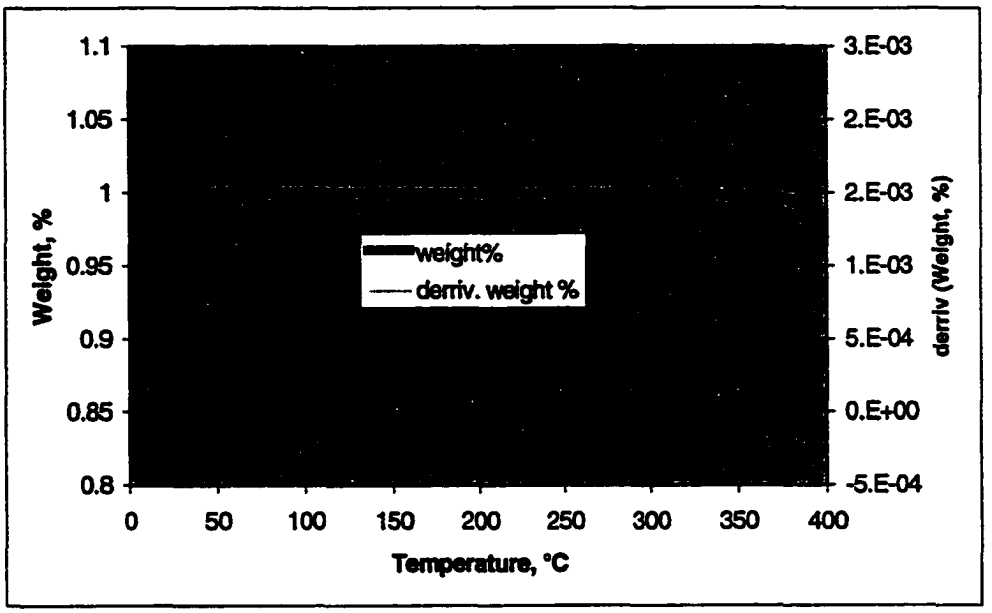

Figure 2.16 b TGA Analysis for HDPE

The same problems can also occur if the holding pressure is applied for an extended time. The proper value for the holding time is correlated with the heat transfer between the cooling part and the mold. Relieving the holding pressure too soon does not prevent shrinkage, while applying pressure on a part that has already solidified leads to overpacking and residual stress. The actual values for back-pressure, and for holding pressure and time were determined empirically and are shown in table 2.2.

The design of the PMMA part and of the mold took into account the properties of PMMA both as melt and as solid. The following design criteria were considered when building the part/ mold:

- PMMA has a high melt viscosity. In order to minimize pressure loss upstream from the mold cavity due to large viscous forces, the mold design requires a large cross-section for the sprue. The sprue was built with an exit diameter of 10 mm;
- Also to preserve maximum melt pressure, a runner-less, gate-less design was chosen where the exit from the sprue feeds directly into the entrance into the mold cavity. This design avoids pressure losses along runners and gate, maximizing the pressure available for forcing the melt into the microstructures;
- High holding pressures can lead to overpacking, and together with the uneven part cross section it can cause sink marks at the sprue gate on the pattern side of the part. To avoid problems in extracting the sprue due to overpacking, a wide taper angle was used for the sprue, 3.5°/side. To avoid the sink marks in the pattern area, the sprue was located on the side of the plastic part, close to the edge, as seen in figure 2.17;
- Simple and efficient separation of the molded part from the mold insert is desirable. The separation is done by a translational movement of the two surfaces away from each other, parallel at all times. A retention ring was designed to hold the part on the stationary plate side upon demolding, and to easily detach to free the part when molding was complete. The retention ring is shown in figure 2.8, together with the stationary mold plate;
- When molding into micropatterns, the advancing melt front will trap air inside the microstructures causing incomplete penetration. Thus, the cavity has to be evacuated prior to injection. The sealing of the cavity for vacuum application was done using a high-temperature o-ring between the mating faces. In addition, the

vacuum system included a vacuum port designed to prevent melt suction inside the vacuum line. The port was positioned inside the mold cavity diametrically opposite from the sprue, and it was designed with a sintered metal (stainless steel) diaphragm as interface between the cavity and the vacuum line. The average pore size of the sintered metal diaphragm is on the order of 2 microns. The location of the vacuum port is indicated in figure 2.18;

Figure 2.17 Conceptual Drawing of Injection Molding Part

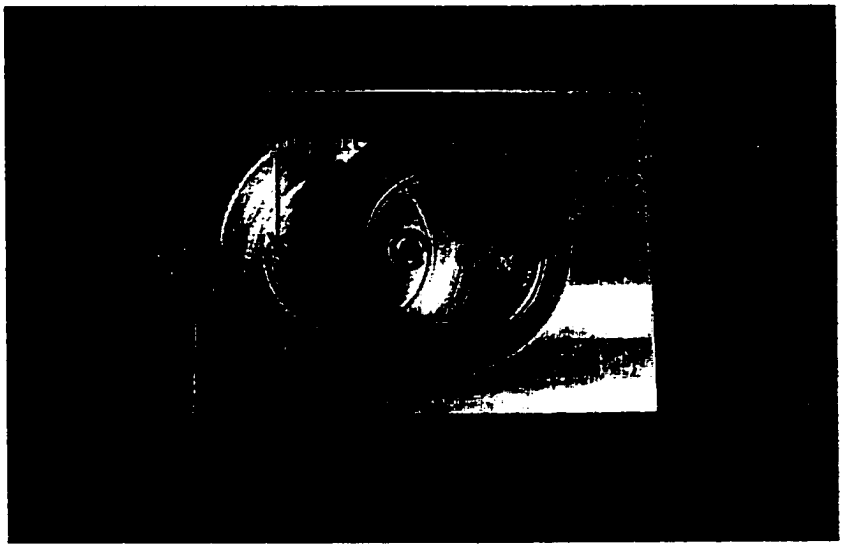

Figure 2.18 Photograph of Stationary Plate with Retaining Ring

- Because PMMA is rather brittle, undercuts in the part will break upon demolding. Thus, the design of the part was done to avoid undercuts other than the retaining

Table 2.2 Summary of Requirements for Injection Molding of PMMA

Drying of the PMMA pellets	PMMA absorbs about 0.4% water. Molded parts are affected by high moisture content, which leads to streak marks on the surface of the part. A material with very high moisture content will mold with bubbles inside the part. Drying is done in an air oven at 70-75 °C for 4 –8 hours. Also, a desiccant can be used to dry out the pellets, but drying time is longer. The moisture content should be below 0.1%
Melt preparation	PMMA is rather sensitive to high shear forces. The heat generated by shearing inside the barrel can degrade the polymer and lead to decomposition into monomer (methylmethacrylate). To prevent this, the dosing is at low screw turning speeds, 5 m/min. Also, to prevent volatiles from escaping the melt, a relatively high backpressure is applied when dosing, 150 bar. A vented barrel is recommended when generation of gaseous compounds cannot be avoided. Holding pressure was applied over 40 sec holding time. The pressure profile was increasing linearly with time, from 50 to 300 bar

Table 2.2. Continued

	The temperature field along the barrel is important to obtain a proper melt. Too low of a temperature can lead to grinding of the pellets and the formation of fine particles which will not plasticate properly. Also, a low temperature will lead to a very viscous melt, which, upon shearing, will generate more heat and lead to monomer generation. It was found that a raising temperature profile along the barrel, e.g. 260- 270-280 °C from feed zone to nozzle, was appropriate.
Mold design and manufacture	Because PMMA is rather brittle compared to other molding plastics, the mold design should avoid undercuts and sharp corners. It is recommended that the sprue have a taper of 3-4° per side to facilitate sprue extraction. The diameter of the sprue can be 8-10 mm, when using a sprue-gate design. The optical properties of PMMA can be easily lost if the surface finish of the mold is not very high. Thus, the mold needs to be well polished to a mirror-like finish for the part to be optically clear. The mold cavity should be under vacuum upon injection, thus a vacuum system has to be fitted on the mold.

- edge. Also, the lateral surface of the cavity was machined at a positive angle of taper, favoring demolding. Also, the part was designed with rounded mating edges between sprue and the part itself, to increase strength.
- Extended residence times inside the barrel aggravate the degradation of PMMA when the melt is prepared at high temperatures. To avoid long residence times, the part was calculated to use about 85% of shot size, at the expense of perfectly accurate shot size preparation. Although accurate shot size dosing is important- especially for smaller parts, in our design we did not observe any negative influences on the quality of the molded parts.

2.6 Repeatability Reproducibility Study for LIGA Micromolding

The process of injection molding involves many repetitions of the same procedure, sometimes for thousands of times. It is then understandable why one is concerned with the performance of the molding process in terms of:

- Molding plastic parts that accurately reproduce the geometry of the mold, and
- Molding plastic parts that have the same characteristics (geometry and physical properties) indifferent of the number of molding cycles.

The mold contains a metallic master (mold insert) patterned with the negative image of the plastic part. After the polymer fills the mold, it hardens and the plastic part is extracted from the mold having the desired geometry- the "negative" image of the mold insert pattern. Upon molding, the resulting plastic parts will differ slightly from the master and among themselves. The mass of polymer undergoes shrinkage and the difference from the mold dimensions will vary around an average value.

For quality control, the molding industry uses control charts to monitor if the performance of a certain molding process lies between acceptable prescribed limits. A control chart consists of a central line representing the average value of the dimension of interest (specifications line), and two control limit -upper and lower- lines (UCL and LCL, respectively), placed equidistant on either side of the central line as depicted in figure 2.19. The distance at which the UCL and LCL lines are positioned relative to the specification line is determined during the product/process development stage. When controlling the quality of the molding process, a prescribed number of parts are sampled from the pool of all molded parts, at various times. The parts are measured, and sample averages are plotted as a time series on the control chart.

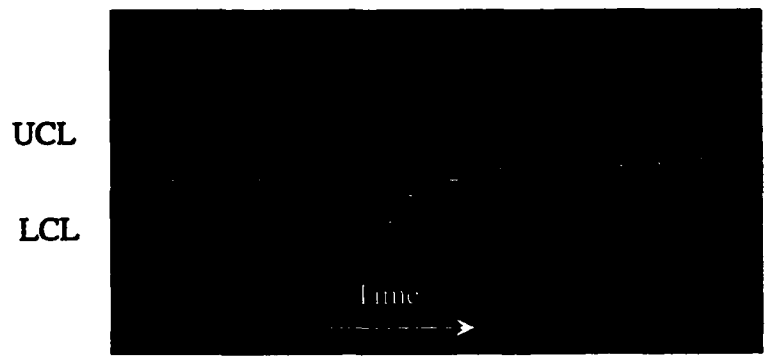

Figure 2.19 Control Chart

This way, two occurrences are monitored on a control chart: variations of the sample average around the specification line and shifting trends above or below the line, both as a function of time. For the control chart in figure 2.19, a random variation within the UCL and LCL is observed to the left of the dashed line. On the same control chart, a shifting trend can be seen occurring to the right of the vertical line.

To keep the scatter at a minimum, the molding process is run keeping as many variables as possible constant. The variables can be process-related, e.g. temperatures,

flow rates, pressures, etc, and material-related such as viscosity, humidity content, etc. Ideally, the identification of all variables influencing the process is done during the investigative research efforts. Keeping these variables constant during the molding cycle would leave the variation of the process to exhibit only naturally random departures from the specifications line. Such a process is called to be under statistical control [17]. When designing a plastic part, the manufacturer and the customer require that certain dimensional specifications are met, but they allow for an acceptable interval of variation. For example, a micropart could be specified to have the wall 625 microns thick, ±5 microns. The values such as ±5 microns are usually a tradeoff between "what can be molded" and "what needs to be molded". While "what needs to be molded" is a result of the micropart design, "what can be molded" is determined experimentally. In a planned set of experiments, the researcher determines the amount of scatter for the dimension of interest when the process is run keeping a comprehensive set of process variables constant. Thus, in the product/process development stage, the distance at which the UCL and LCL lines of a control chart are positioned relative to the central line is determined. This distance is based on the standard deviation or on the range (difference between the largest and the smallest value) for the measurements of the dimension of interest, as it will be calculated later in this section. Also during the product/process development stage, the average departure of the measurements from the central line is determined. For instance, the amount of shrinkage is determined when the dimensions for the plastic part are compared with the dimensions on the metallic insert.

During the production phase, the control chart is used to monitor the performance of the process. An increase in the amount of variation around the central

value indicates that a parameter is out of control and that it varies randomly. For instance, if the mold temperature cannot be maintained at a constant level due to a malfunction in the control unit, the part shrinkage will vary since the shrinkage is proportional to temperature. When the UCL or LCL limits are exceeded, the molding is stopped and the problem is fixed to bring the process back under statistical control. Secondly, a shift in the average of the measured values indicates that a certain parameter has changed to a new constant value, for instance the quality of the feedstock has changed leading to a new value of the part shrinkage. Again, the molding is stopped and an adjustment is made to bring the process back under statistical control.

This section reports on the transfer and preservation of geometrical characteristics of HARMs molded by injection molding, when the variables injection speed, mold temperature and barrel temperature are kept constant. In the following paragraphs, the terms *repeatability* and *reproducibility* will be used to describe variations of the sample average around the specification line and shifting trends above or below the line, respectively. The study of reproducibility and repeatability is part of the effort to bring a process under statistical control [17]. The terms are borrowed from the statistical field of gauge measurements evaluation [18]. In this section, we will use *reproducibility* as a term describing how much a plastic micropart is different when compared with the metallic master used for replication- mold insert. In addition, we will use *repeatability* to describe how much plastic microparts molded under the same conditions differ from each other. On a control chart, reproducibility would correspond to identification and quantification of shrinkage, while repeatability would indicate the random variation around the centerline.

The importance of injection speed and mold temperature and barrel temperature on the quality of the molded microstructures was reported in section 2.4. In this section, the process of micromolding is studied for reproducibility and repeatability under constant injection speed, mold temperature and barrel temperature. Specifically, a micro heat exchanger pattern was molded, under constant conditions, using PMMA. The pattern consists of three columns of fine rectangular troughs. Each trough is about 80 microns thick and 1000 microns deep, as shown in Figure 2.20.

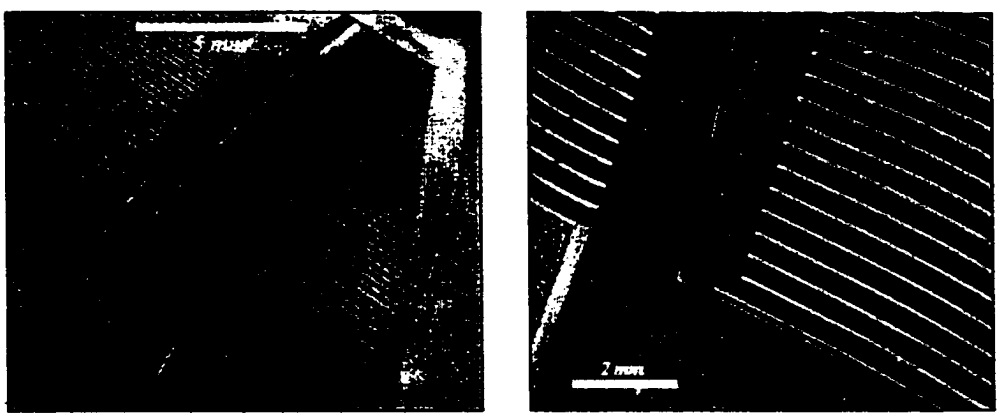

a b

Figure 2.20 SEM Micrograph of: a- metallic master (mold insert), and b- molded pattern

2.6.1 Repeatability

For the study of repeatability, 27 plastic parts were produced by injection molding. The experimental design consists of the following: molding runs were performed in three different batches corresponding to three different days; in each day (batch), three plastic parts were molded; the surface of a part was then divided in 3 smaller rectangles, corresponding to the columns of microchannels. Each resulting rectangle was uniquely identified by its vertical location: west, central, or east. For each individual rectangle, twelve microfins were randomly selected and their thickness was

measured. This was repeated for every molded part. Thus, the experimental design consisted of the following factors:

- batch, with three levels $i = 1, 2, 3$
- part, with three levels $j = 1, 2, 3$
- position, with 3 levels $k = 1, 2, 3$

The levels of the "position" factor are defined by the column locations (West, Central, East). The purpose of designing the experiment with three different days of operation and small number of parts manufactured in one day was to identify the presence of influences due to small series production (frequent machine start/stop cycles). A sample of 6 of the total of 324 fin thickness measurements is given in Table 2.3.

Table 2.3 Sample of Thickness Measurements

1	1	West	70
1	1	West	70
1	1	West	71
1	1	West	70
1	1	West	72
1	1	West	74

The mathematical model describing the potential sources of variation for an individual thickness measurement (effects model) is:

$$y_{ijkl} = \mu + \beta_i + \rho_{j(i)} + \alpha_{k(ij)} + \varepsilon_{ijkl} \quad (15)$$

where:

- y_{ijkl} is the thickness of an individual fin
- μ is the overall mean for all fins measured

- β is the contribution of the "batch" effect
- ρ is the contribution of the "part" effect
- α is the contribution of the "position" effect
- ε is the random error term.

The statistical analysis of the thickness measurement data was performed using the SAS® package. The above model was used in a General Linear Model (GLM) procedure where differences between batches, parts, and regions were assessed based on Tukey's post-ANOVA comparison technique. Table 2.4 shows the output of the GLM procedure for each effect. As seen, the p-values indicate that the null hypothesis of equal means cannot be rejected in the case of the "batch" (p=0.2844) and the "part" (p=0.997) factors. In the case of the "region" factor, at least one mean is different and the null hypothesis of equal means is rejected (p=0.0001).

Table 2.4 Output From the GLM Procedure

Source: BATCH
Error: MS(SAMPLE(BATCH))

DF	Type III MS	Denominator DF	Denominator MS	F Value	Pr > F
2	12.114197531	6	7.7561728395	1.5619	0.2844

Source: PART(BATCH)
Error: MS(REGION(BATCH*SAMPLE))

DF	Type III MS	Denominator DF	Denominator MS	F Value	Pr > F
6	7.7561728395	18	196.08024691	0.0396	0.9997

Source: REGION(BATCH*PART)
Error: MS(Error)

DF	Type III MS	Denominator DF	Denominator MS	F Value	Pr > F
18	196.08024691	297	2.1966891134	89.2617	0.0001

Statistically speaking, these results indicate that the factors "batch" and "part" do not influence the value of the thickness of the fins. Thus, the thickness of the molded

fin is not a function of the day when the part was molded nor is it a function of the molded part on which the fins were located. However, the thickness of the fins is a function of the position (region) on the plastic part.

At this point, the calculation of LCL and UCL limits for the process is done, based on the standard deviations for each location. Table 2.5 contains the values of the statistics used in the LCL UCL calculations, based on fin measurements taken on each region on the molded parts. The following formulas are used:

$$UCL = Mean + 3 \cdot \sqrt{SD^2/n} \qquad LCL = Mean - 3 \cdot \sqrt{SD^2/n} \quad (16)$$

Table 2.5 Means and Standard Deviations for the East, Central, and West regions

E	108	80	1.21
C	108	76	1.74
W	108	72	1.69

The UCL and LCL values have the following statistical interpretation: when taking a sample of n measurements, their average will fall between the LCL and UCL limits with a probability of 97%. The value of n in our case is chosen to be 5. Assuming an average value of the standard error SD=1.54, the calculation becomes, for the CENTRAL region:

$$UCL = 76.3 + 3 \cdot \sqrt{1.54^2/5} \cong 78 \qquad LCL = 76.3 - 3 \cdot \sqrt{1.54^2/5} = 74$$

Based on these values, we can now predict that for instance, for the Central region, the average fin thickness will be 76 ± 2 microns for the case when samples of 5 measurements would be taken for statistical control. Table 2.6 shows the Upper Control Limit and Lower Control Limit for all 3 regions WEST CENTRAL and EAST.

Table 2.6 UCL and LCL Values for the Thickness of Molded PMMA Microfins

E	80	82	78
C	76	78	74
W	72	74	70

2.6.2 Reproducibility

The results of the analysis performed on the thickness measurements indicate that the only factor affecting the variability of the fin thickness is the "region" factor. Thus, we can conclude that the fins have different thickness based on their position on the plastic part. Moreover, Table 2.7 shows comparisons between the 3 regions, based on the Tukey's adjustment method; p-values below 0.05 indicate that any two cross-classified averages are different from each other.

Table 2.7. Pairwise Comparisons for the Average Fin Thickness

Region	Average	i/j	1	2	3
c	76.3518519	1	.	0.0001	0.0001
e	80.5277778	2	0.0001	.	0.0001
w	72.5185185	3	0.0001	0.0001	.

All pairwise comparisons resulted in p-values of 0.0001, indicating that the average fin thicknesses for all three regions are different from each other. A plausible explanation for the difference in average fin thickness between regions can be the existence of similar differences between the average dimensions of the micro-troughs on the mold insert.

To test this hypothesis, the width of the micro-troughs on the mold insert into which the fins were molded was measured. The surface of the mold insert was divided into 3 rectangles based on the same geographical arrangement as in the case of the plastic parts. Twelve measurements were taken for each of the 3 rectangles (geographical positions), resulting in a total of 36 measurements. Table 2.8 shows the actual values of the gap widths. The data in Table 2.8 was then used in a statistical analysis identical with the one performed for the molded parts data.

Table 2.8 Microgap Widths as a Function of Geographical Location

1	WEST	76	13	CENTRAL	76	25	EAST	83
2		75	14		75	26		84
3		73	15		82	27		83
4		76	16		78	28		83
5		74	17		81	29		87
6		72	18		79	30		84
7		77	19		84	31		83
8		79	20		79	32		83
9		76	21		81	33		80
10		77	22		79	34		81
11		75	23		83	35		82
12		75	24		80	36		83

The results are presented in Table 2.9.Again, the p-values lower than 0.05 indicate that the two means under comparison are statistically different.As seen from Table 2.9, the averages for all three regions, WEST, CENTRAL, and EAST on the insert are different from each other.

Table 2.9 Pairwise Comparisons for Microgap Width Measurements

Region	Average	i/j	1	2	3
C	79.7500000	1	.	0.0019	0.0001
E	83.0000000	2	0.0019	.	0.0001
W	75.4166667	3	0.0001	0.0001	.

In order to quantify the reproducibility for the process of micromolding, the thickness of the molded fins must be compared against the width of the microgaps into which these fins were molded. The comparison between these average values can be done by subtracting average values per region; thus three differences d_W, d_C, and d_E can be calculated. Moreover, a better descriptor of reproducibility is obtained when these values are reported as percent dimensional change (shrinkage):

$$\%shrinkage = \frac{d}{width_{insert}} \times 100 = \frac{width_{insert} - thickness_{plastic}}{width_{insert}} \times 100$$

resulting in three shrinkage values s_W, s_C, and s_E. The homogeneity of these s-values is then evaluated. Similar values for s_W, s_C, and s_E would indicate a homogeneous shrinkage for all regions. The comparison insert vs. plastic is in table 2.10.

Table 2.10 Shrinkage Values for Each of the Three Geographical Regions

ORIGIN	MEAN	% SHRINKAGE
Metallic insert	83	3.61
Molded plastic part	80	
ORIGIN	MEAN	% SHRINKAGE
Metallic insert	79	3.79
Molded plastic part	76	
ORIGIN	MEAN	% SHRINKAGE
Metallic insert	75	4.0
Molded plastic part	72	

2.6.3 Conclusions on Repeatability and Reproducibility

The study of repeatability and reproducibility for the process of injection molding of HARMs was performed to investigate the stability of the process during small series production (often machine start/stop cycles). The analysis was performed by means of statistical interpretation of the measurements taken on both the metallic master (mold insert) and the molded parts. In the repeatability study, we took into account three factors that could influence the variation of fin thickness: batch-or the day when parts were molded, part- the plastic part onto which the fins were molded, and region- the geographical location of the fin on the plastic part. The results of the repeatability study indicate that there is no variation in the thickness of the microfins due to the day when the part was molded or due to the part itself. Statistically speaking, all the parts molded in our study were identical. This corresponds to a high degree of *repeatability* for the molding process. UCL and LCL limits were calculated for samples of 5 measurements.

Secondly, the results of the analysis performed on the thickness measurements indicate that the only factor affecting the variability of the fin thickness is the "region" factor. In other words, all parts molded where identical, but for all parts, the fins have different thickness based on their position on the plastic part. Next, we investigated to see if the same location-dependent variation exists for the width of the gaps on the mold insert into which the fins were molded. The statistical analysis indicated that the same geographical variation exists on the mold insert, too: the microgaps had different thickness as a function of their position on the insert.

Thirdly, the thickness of the fins was compared with the width of the gaps on the mold insert. The comparison yielded a coefficient of shrinkage that has homogeneous

values for all three geographical locations, with an average value of 3.6%. This relatively high average shrinkage value can be explained by the application of insufficient holding pressure during the cool-down period of the molding cycle. After the mold cavity has been filled completely, the polymer starts to solidify thus shrink.

This amount of thermal shrinkage is estimated as the sum of shrinkage of the melt between injection temperature and Tg, and shrinkage of the solidified part between Tg and the demolding temperature:

$$\%shrinkage = \alpha_{melt}(T_{melt} - T_g) + \alpha_{solid}(T_g - T_{demold}) \qquad (17)$$

For PMMA, when T_{melt}=200°C, Tg=90 °C, and T_{demold}=35 °C, the predicted shrinkage is around 5%. To minimize shrinkage of the molded part during cool-down, polymer melt is forced continuously into the cavity to maintain the same specific volume in the melt as in the solid state. This is done by the application of the so-called holding pressure. The experimental shrinkage value of 3.6% is probably due to the application of insufficient holding pressure following cool-down.

2.7 Conclusions Injection Molding

Experimental work was carried out to study the microreplication of high aspect ratio microstructures (HARMs) by means of injection molding. The general conclusion of this work is that injection molding of HARMs follows the principles of injection molding of larger scale parts. However, several specific considerations separate the injection molding of HARMs from the existing macro-scale molding applications. First, heat transfer and flow issues become more critical in the case of micro-scale high aspect ratios. This is due to the very narrow widths into which the melt has to penetrate; the heat transfer between the polymeric melt and the surroundings is intense, and the

pressure losses associated with the flow into these narrow spaces are high. Molding experiments were performed to evaluate the importance of injection speed and mold insert temperature as variables for injection molding of HARMs. It was found that the temperature of the mold insert is determinant, followed by injection speed. Heating the mold insert to a temperature corresponding to the melting point of the polyethylene used in injection led to complete penetration between the microposts used as test pattern. This held true for any value of the injection speed, although increasing the injection speed did favor the process at lower mold insert temperatures.

Secondly, the injection machine employed for this research work was a commercially available machine designed for generic molding applications. Therefore, several specific adaptations and modifications were made to the injection machine in order to make it suitable for micromolding. A vacuum system was added to evacuate the mold cavity, and a heating/ cooling system was mounted on the insert side of the mold. Also related to the hardware, the design criteria for building the mold included minimizing the pressure losses upstream from the mold cavity, a uniform cross section of the melt path, and a proper retaining mechanism for separation of the molded part from the mold insert.

Thirdly, materials used for injection molding HARMs were either semi-crystalline or amorphous. As an example of a semi-crystalline polymer, high density polyethylene was used as a molding material having good flow characteristics. Molding materials need to be analyzed prior to molding to determine the flow characteristics as a function of temperature and imposed shear rates. Special care needs to be used when molding PMMA due to its susceptibility to rapid degradation over 300 °C.

Last, experiments were carried out and statistical analysis was performed to study the repeatability and reproducibility limits for injection molding of LIGA HARMs in a micro heat exchanger pattern. The study found that the process of injection molding of these HARMs was repeatable. The study of pattern reproducibility showed a rather large value for the dimensional change of the molded microfeatures, compared to the mold insert. This shrinkage value was explained based on insufficient application of holding pressure after injection.

CHAPTER 3. HOT EMBOSSING

3.1 Survey of Embossing Techniques

Hot embossing is a molding technique consisting of patterning a polymeric substrate by pressing the heated metallic insert into the moldable plastic. The technique involves the use of a molding material in form of a preshaped sheet or in form of a powder, which can be molded under applied pressure and heat. Bacher et al. describe the process of hot embossing using either a solid film (produced by casting of a mixture MMA/PMMA) or a pile of powder-like PMMA [2]. The material was positioned either underneath the mold insert (when a film was used) or on top of the insert (when powder was used). The PMMA was heated "beyond its glass transition temperature" and structured under vacuum by impression of the hot molding tool [2]. Harmening et al [11] report on their work with hot embossing mentioning that the quality of the final product is influenced by the mold release agent used during the process, together with the molding and the "unmolding" (demolding) temperatures. Five different experimental schemes were presented [21] based on the type of the material used and on the way the material was positioned with respect to the molding tool.

The German company Jenoptik has developed the HEX hot embossing system, as a result of the extensive experimental work carried out over more than ten years of research. One of the features incorporated into the system is a high alignment precision (10microns over 120 mm of span) of the two plates of the press. Also included as standard features are a precise control of the temperature of the plates and an accurate control over the clamping force and speed. The two plates are enclosed inside a vacuum chamber that allows for evacuation of the molding area prior to the actual embossing

step. The maximum molding force is 200 kN, while the maximum molding temperature is at 320 °C. The system is computer controlled and fully integrated. Parts embossed using this system include micro-optical parts and microfluidic devices [19].

One other technique used to produce very fine structures, somewhat related to hot embossing, is in-mold casting. This technique also deals with a reacting mass of prepolymerized reactants [20, 21] which is simply poured into a master pattern. After casting, the hardened material is separated from the master by peeling it off. Using an elastomeric master rather than a rigid one substantially eases the process. The procedure was applied to first produce an elastomeric master made of poly(dimethylsiloxane), PDMS . The prepolymerized PDMS was cast against an original master which had been patterned with nanometer-size structures using lithographic techniques; this original master could be SiO_2, Si_3N_4, metals or PMMA. The resulting elastomeric master was in turn used to pattern a rigid organic polymer, for instance photochemically curable polyurethane, PU [21]. This in-mold casting, also called replica molding, of PU against a PDMS master could also be carried out while the PDMS was bent mechanically; in this case smaller features than on the original master could be produced.

3.2 Theoretical Considerations

In order to better understand hot embossing and to identify the important operating variables for this technique, one can approach the process through the simplified model of squeezing flow between two plates (disks). Leider and Bird [25] reviewed various solutions for squeezing flows between two disks, concluding that a steady state solution for a power-law fluid is satisfied for the case of "slow" squeezing of melts. Tadmor and Gogos [25] present the derivation of the Scott equation for such

flows, as follows. For the geometry presented in figure 3.1, in cylindrical coordinates, the power law model can be written as:

$$\tau_{rz} = m\left(-\frac{dv_r}{dz}\right)^n \quad (1)$$

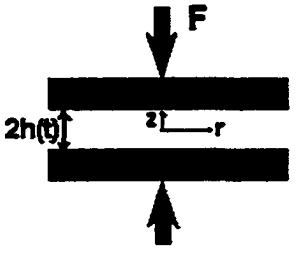

Figure 3.1 Schematic diagram of squeezing flow between disks. Origin of the cylindrical coordinate system is placed midway between the disks.

Assuming no net flow in the angular direction, the equation of continuity is reduced to:

$$\frac{1}{r}\frac{\partial}{\partial r}(rv_r)+\frac{\partial v_z}{\partial z}=0 \quad (2)$$

Neglecting gravitational effects, the r-component of the equation of motion is simplified to:

$$\frac{\partial \tau_{rz}}{\partial z} = -\frac{\partial P}{\partial r} \quad (3)$$

The boundary conditions are:

$$v_r(h)=0 \quad (4)$$

and, for reasons of symmetry, $\frac{\partial v_r}{\partial z}=0$ at $z=0$ (5)

Equation 2 can be integrated to give:

$$\int dv_z = -\frac{1}{r}\int_0^h v_r dz \quad (6)$$

which can be rewritten as:

$$\frac{1}{2}\dot{h} = -\frac{1}{r}\int_0^h v_r dz \qquad (7)$$

where $\dot{h} = \frac{dh}{dt}$ is the instantaneous vertical velocity of the plates.

Combining equations 1 and 3 and integrating yields:

$$v_r = \frac{h^{1+s}}{1+s}\left(-\frac{1}{m}\frac{dP}{dr}\right)^s\left[1-\left(\frac{z}{h}\right)^{1+s}\right] \qquad (8)$$

The expression for velocity in equation 8 is used in equation 7 in conjunction with equation 3 and the power-law model to obtain the expression for differential pressure:

$$\frac{dP}{dr} = -m\left(\frac{2+s}{2h^{s+2}}\right)^n\left(-\dot{h}\right)^n r^n \quad (9)$$

which is integrated to obtain the radial pressure distribution at any value of h:

$$P = P_a + m\frac{(2+s)^n}{2^n(n+1)}\frac{\left(-\dot{h}\right)^n R^{1+n}}{h^{1+2n}}\left[1-\left(\frac{r}{R}\right)^{1+n}\right] \quad (10)$$

From equation 10, the closing force at constant closing speed is obtained by integrating over the disk surface:

$$F_N = m\pi\frac{(2+s)^n}{2^n(3+n)}\frac{\left(-\dot{h}\right)^n R^{3+n}}{h^{1+2n}} \qquad (11)$$

This is the Scott equation, which can be integrated for $h(t)$:

$$\frac{h(t)}{h_0} = \left[1+\frac{2(1+s)(3+n)^s}{2+s}\left(\frac{F_N}{m\pi R^2}\right)^s\left(\frac{h_0}{R}\right)^{1+s}t\right]^{-n/(1+n)} \qquad (12)$$

where h_0 is the initial half-gap between disks, n is the power law flow index, m is the consistency, $s = \frac{1}{n}$, and R is the disk radius. The half-time value, that is the time

needed for reducing the gap to one-half the initial value can be obtained from equation (12):

$$t_{1/2} = K\left(\frac{m\pi R^2}{F_N}\right)^s\left(\frac{R}{h_0}\right)^{1+s} \qquad (13)$$

where

$$K = n\left(\frac{2^{1+s}-1}{2n}\right)\left(\frac{2+s}{1+s}\right)\left(\frac{1}{3+n}\right)^s \qquad (14)$$

Bird notes that the Scott equation is applicable for "slow" squeezing of melts [4]. Slow squeezing rates allow for the relaxation of visco-elastic effects through long experimental times. This helps to avoid phenomena related to stress overshoot where the polymer is not allowed to "catch-up" with the imposed signal. Therefore, at a given temperature, experiments carried out at low values of the Deborah number will conform to the Scott equation. Low *De* values (smaller than or equal to one) allow stress relaxation to occur during embossing, leading to permanent deformations of the thermoplastic polymer subjected to compression. Deborah number is defined as:

$$De = \frac{\lambda}{t_{exp}} \qquad (15)$$

where λ is the characteristic relaxation time and t_{exp} is the experimental time.

Equation 12 shows which variables will be involved in the squeezing flow. The geometry of the flow can be generalized to include a set of N individual pairs of disks of radius R pressed together at the same time in the same press. This scenario is a qualitative descriptor of the case of hot embossing of microstructures. Thus, after pooling together all constants in equation 12, the expression can be rearranged to give:

$$\left(\frac{h}{h_0}\right)^{1+s} = 1 + K(F)^s\left(\frac{1}{N}\right)^s\left(\frac{1}{e^{-AT}}\right)^s\left(\frac{1}{R}\right)^{3+s} t \quad (16)$$

where K and A are constant, and T is the temperature of the melt, assumed uniform. The temperature exponential in equation 15 is introduced because for most thermoplastics an increase in temperature decreases the value of consistency m according to an Aarhenius type relationship $m(T) = m_0 \exp(-A \cdot T)$.

From equation 16 it follows that, for a given geometrical setup (given N and R), the value of the gap h depends on force, temperature and embossing time. It can be seen that a change in temperature has the most dramatic effect on the value of h, followed by a change in force F (since $s = \frac{1}{n} > 1$) and a change in duration t. Elevating the temperature of the polymer will facilitate the squeezing of the polymer, but with upper restrictions related to material stability and duration of the embossing cycle. The temperature cannot be increased over the stability limit of the polymer used, otherwise the polymer will be "burned" and degradation will occur. Also, too high of a temperature will lead to an increase in cycle time since the embossed part needs to be cooled prior to separation from the insert. Moreover, in many cases, an elevated temperature combined with a long contact time will promote adhesion between the polymer and the metallic insert, making demolding more difficult. To prevent such negative temperature-related effects from occurring, an increase in compression force F can be used to facilitate squeezing of the plastic. The limitation in this case is due to the embossing machine, which should be capable of the required force output. Last on the list of parameters is embossing time t. The longer the force F is applied to compress the two disks, the smaller the separation gap between disks. As discussed above, the value

of *t* needs to be long enough to eliminate stress overshoot and to allow for relaxation of the molecular chains under stress thus allowing for permanent deformation of the substrate. The upper limit of cycle duration is related to the aforementioned problem of stiction and to the economics of the overall cycle time.

3.3 Hot Embossing Equipment

The hot embossing work presented here was performed using a high-precision press, model TS21HC manufactured by PHI, Ca. This press model is manufactured for applications requiring independent control of pressure, temperature, and parallelism of the plates. However, this press was not designed specifically for hot embossing of HARMs, and additions were made to adapt it to the scope of microreplication, as it will be later discussed in detail. The plates of the PHI press are 8 inches x 8 inches, supported on four sliding posts. The sliding posts are chrome-plated, and the bottom plate slides up and down on linear bushings for low-friction closing. An air-over-hydraulic cylinder, capable of a maximum force of 9000 N, provides the closing force. The two plates have a parallelism of 8.5 microns over 100 mm of span. The PHI press is also designed with a heating/cooling system. The heating can be controlled independently for each of the upper and lower plates at a rate of approximately 13 F/min, while the cooling is done simultaneously for both the upper plate and the lower plate. The closing speed can be adjusted to achieve values of 50 microns/sec, minimum, but with reduced accuracy. Table 3.1 below compares the principal characteristics of the PHI system with the Jenoptik HEX 03 system. HEX is a series of embossing machines designed specifically for micro hot embossing, and HEX 03 is the largest model in the

series [26]. Different from the HEX 03, the PHI press does not have a vacuum chamber, and most of the controls are separated from each other and are not computer controlled.

Table 3.1. Comparison between Jenoptik and PHI Embossing Systems

Press force	Adjustable ≤ 200 kN	Adjustable ≤ 8900kN	
Embossing time	Cycle time (typical) 7 min	1-10 min	
Temperatures	Heating-up time (60°C to 180°C) < 7 min Cooling period (180°C to 60°C) < 7 min Temperature inside of the chamber ≤ 320 °C Temperature stability ± 2 K	< 15 min < 7 min ≤ 250°C N/A	Cooling for PHI system is simultaneous for both plates
Vacuum	Vacuum / chamber (oil-mist free) ≤ 1 mbar Pump-down time ≤ 1 min Vent time ≤ 0.5 min	≃ 0.1 bar ≤ 5 sec ≤ 5 sec	Vacuum chamber designed separately and added to the PHI system
Work substrates	Max. substrate size Ø150 mm or Max 150 mm x 150 mm. Embossing area Ø 120 mm Permissible thickness of the emboss sandwich (contains mold and workpiece material) 1...20 mm Adjustment of the vacuum chamber to the sandwich level automatically	Ø133 mm N/A Ø 120 mm 1...12 mm Yes	
Alignment unit	Max. distance between alignment markers 90 mm Instrumental overlay accuracy ± 3 µm	N/A	
Cooling Water	Inlet temperature ≤ 15°C Water consumption 6l/min	From water line	

Table 3.1 Continued

Electrical supply	230 / 400 VA, Frequency 50 Hz or 60 Hz Power consumption 16.0 kW	120 VAC 2.6 kW	
Pneumatic connection	Compressed air 0.6 MPa...0.8 MPa	0.5Mpa min.	
Dimensions	Width 2600 mm Depth 900 mm Height 1800 mm	812mm x 406mm x 812mm	
Weight	Total weight approx. 1700 kg	120 kg	

Because the PHI system is designed as a general-purpose hot-plate press, a vacuum chamber was designed and built to make the press suitable for hot embossing of microstructures. The design of the vacuum chamber was done based on the following criteria:

- Employment of a standard mold insert geometry. This criterion was imposed as part of the effort to facilitate rapid inter-use of inserts between injection molding and hot embossing. The standardization was done by deciding on a circular insert geometry, having a diameter of up to 4 ¾ inches, with the pattern inscribed inside a 3 ½ inches diameter circle;
- The need for an automated demolding mechanism. Demolding from the metallic insert has to be done by separating the substrate from the insert parallel to each other, without lateral movement that can deform or break the microfeatures. This requirement can be fulfilled if the demolding is done automatically, without manually handling of the substrate;
- Maximum height of the molding sandwich (mold insert and molding substrate) up to ½";

- Preservation of plate parallelism;
- Control of temperature through the press heating/cooling system.

Applying these criteria, the design resulted in the vacuum chamber consisting of a piston/cylinder assembly, with the sealing done using an o-ring mounted on the moving piston. The top of the piston is secured onto a square support plate, while the cylinder is attached to its own square support plate. These two halves of the so-formed sealed chamber are aligned relative to each other by a set of four sliding posts machined to tightly fit into corresponding cups. The alignment posts are screwed into the support plate on the piston side, while the cups are screwed into the support plate on the cylinder side, at the corners. To support the piston such that the mold insert does not touch the molding substrate prior to closing the press, a spring is inserted at the bottom of each cup. Figure 3.2 shows a photograph of the piston and of the cylinder composing the vacuum chamber. Also shown on the right side of figure 3.2 is the mold insert mounted on the piston, using six miniature screws # 2-56. This mounting method resulted from the effort to standardize the geometry of the mold inserts to where mold inserts are now easily interchangeable. Both the hot embossing press and the injection molding machine use the same mold inserts, and a minimal time is needed to mount and un-mount the insert inside the vacuum chamber of the hot embossing press or inside the mold cavity on the injection molding machine.

Because the heating and cooling of the two sides of the vacuum chamber is done from the press platens, heat transfer is important. The materials for building the vacuum chamber were required to offer rapid and uniform heat transfer, and to have good machinability and wear resistance. The piston was made of aluminum, together with the

support plates. Aluminum was chosen because it is easy to machine, light, and good heat conductor and leveler.

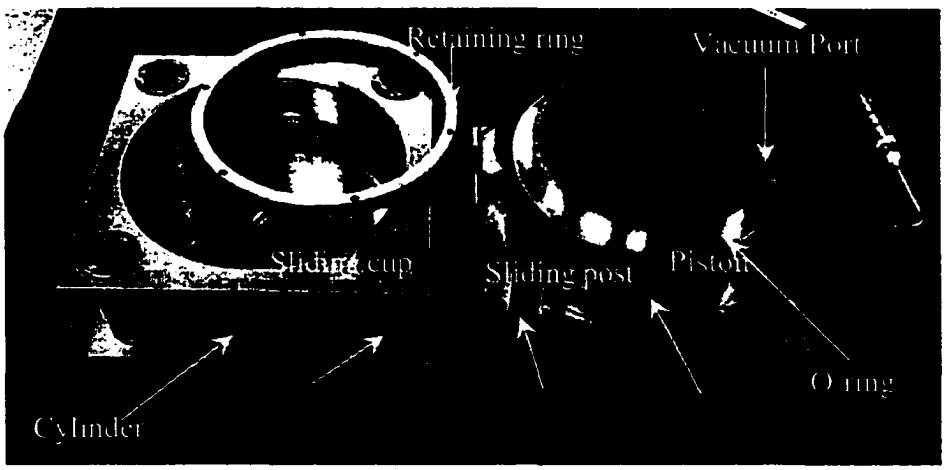

Figure 3.2 Vacuum Chamber Halves: Cylinder and Piston

When heated to 160 °C, the radial temperature gradient on the insert face of the piston was measured to be less than 4°C. On the other side, the disadvantage of using aluminum is its softness: it scratches and it dents easily, which may cause problems with the long-term use of the chamber if careful operation and handling are not employed. When designing the vacuum chamber, the original material for the cylinder was glass, to allow for observation inside the chamber. However, Pyrex glass proved a poor choice due to the mismatch in thermal expansion coefficients, $\alpha_{Al} = 23 \times 10^{-6}/°C$, $\alpha_{Pyrex} = 3 \times 10^{-6}/°C$. As a result, the cylinder was made of steel, which expands at a rate comparable to aluminum, $\alpha_{steel} = 11 \times 10^{-6}/°C$, and it obviously doesn't break as easily as glass. Although it is harder to machine than aluminum, steel is also more wear resistant than aluminum, and this becomes important when considering high-temperature friction due to the traveling of the piston inside the cylinder. When applying the design rules for o-ring grooves, the sizing of the piston and cylinder took into account the difference between the expansion coefficients and the allowable amount of squeeze for the o-ring

inside its groove. The o-ring material was chosen to be a high-temperature silicone rubber capable of withstanding the elevated temperatures along the piston.

3.4 Hot Embossing Experiments

3.4.1 Substrate preparation

The embossing experiments were carried out using commercially available polymers, pre-shaped as 5.3" diameter disks. Before embossing, the molding substrate needs to be prepared to ensure good replication of the microstructures. The preparation is done to clean the substrate of dust and small particles, and also to eliminate the moisture content from the substrate. After removing the protective foil, the substrate was first cleaned by spraying isopropanol on both surfaces and blowing it dry. It was found that this cleaning method is better than wiping the surfaces, because it eliminates the risk of scratching the glass-like surface finish, and it prevents the deposition of electrostatically-charged lint on the surface to be embossed. Drying the substrates was done in an air oven at 80 °C, for 4-8 hours. The substrates were then stored under dry environment inside a desiccator.

3.4.2 Molding sequence

One of the goals of this research work was to establish a standard embossing procedure in order to ensure repeatability for the hot embossing process. The construction of the vacuum chamber, together with deciding on standard mold insert geometry greatly helped in achieving repeatable embossing results. For the embossing experiments presented in this work, a hot embossing sequence of operation was developed to involve the following steps:

- substrate preparation

- substrate mounting
- close vacuum chamber
- place vacuum chamber between the press platens and connect the temperature gage and the vacuum line
- establish desired temperatures for the insert and the molding substrate
- establish vacuum inside the chamber
- close press and emboss
- open press and demold
- disconnect vacuum chamber and remove it from the press
- open chamber and remove the substrate
- flatten substrate

Mounting of the substrate is done using a retaining ring, as shown in figure 3.2. The ring fits around and on top of the edge of the plastic disk, and it has the role to secure the substrate when demolding it from the insert. Securing the ring to the bottom plate of the vacuum chamber is done using six miniature screws. Before closing the vacuum chamber, the mold insert is conditioned using a mold release agent. The mold release agent is used to prevent stiction of the plastic to the insert. The agent used for embossing PMMA and PC was a dry film release, sprayable mixture, containing phosphate esters, polyolefins, and fluoropolymers. This mixture has good heat stability and it forms a layer that does not transfer onto the molded part. When both the mold insert and the molding substrate are ready for embossing, the vacuum chamber is closed, placed between the press platens, and the temperatures are set for both the mold insert and the substrate. The mold insert temperature is set at a value higher than the

glass transition temperature of the thermoplastic used. At the same time, the temperature of the substrate is raised, too, but only to a value lower than T_g. This is done to allow for the desired plastic deformation of the top portion of the substrate, but, at the same time, preserving the shape of the disk. As it was discussed at the beginning of this chapter, the deformation of the polymer during embossing is a function of time, force, and temperature. For a given force, while the mold insert contacts the polymer during the embossing time and at the embossing temperature, adhesion forces are developed between the metal and the plastic. These adhesion forces combined with undesired undercuts on the mold insert, and with friction forces due to mismatch in the expansion coefficients for plastic and metal lead to difficulties in demolding. The magnitude of these unfavorable forces can be enough to cause plastic deformation of the entire substrate upon demolding or it can cause breakage of the molded microstructures, which remain stuck on the insert. Because the substrate has the shape of a disk held in place by the retaining ring, the stiction forces that are exerted centrally cause bowing of the disk with the convexity towards the micropatterned side. This deformation can be recovered entirely after separation, but sometimes it can also be severe enough to become permanent. To avoid such problems from occurring, a combination of lowest possible insert temperature and shortest embossing time should be used. This previous assessment is purely qualitative, since the processing values for embossing time and temperature were only determined experimentally. Another type of permanent deformation of the substrate is induced by the existence of a temperature gradient across the thickness of the substrate. This temperature gradient leads to the formation of a bow in the substrate disk with the concavity towards the micropatterned

side. Although this deformation cannot be avoided when using the PHI press, a post-embossing baking of the part completely eliminates the bow. Thus, after extraction from the vacuum chamber, two molded parts were clamped back-to-back and were placed inside a hot-air oven at 85°C, just below the glass transition temperature of PMMA. The parts were allowed to relax and flatten against each other at this temperature, for 6 hours.

Table 3.3 Example of Embossing Parameters. Pattern: Micro Heat Exchanger. Embossing Substrate Material: PMMA Max. Aspect ratio: 8:1

Mold Insert temperature, °C	180
Substrate temperature*, °C	85
Embossing time, min	7
Embossing force, N	3780
Force raise rate (0-nom.), N/sec	100
Demolding temperature- insert, °C	145
Demolding temperature- substrate, °C	45

(*Measured as temperature of the press platen)

3.4.3 Embossing of PMMA

As mentioned above, the material mostly used for hot embossing of HARMs was PMMA. Several reasons prompted the use of PMMA as an embossing material, related to its optical and mechanical properties, as presented in chapter 2. From the embossing viewpoint, PMMA offers some advantages over other thermoplastics:

- it has a lower Tg than other optically-clear materials such as PC. This makes the embossing process less difficult, because lower temperatures are employed when pressing the substrate. Operating the press at lower temperatures is desirable, because not only the operation of the press and the handling of parts are easier, but also less thermal stress is imposed on the mold insert and vacuum chamber;

- it has good machinability, allowing for relatively easy post-embossing machining. One of the collaborative goals of this research was to successfully manufacture a cross-flow micro heat exchanger. The manufacture of this part involves several post-embossing machining steps, as it will be shown in the following paragraphs, and PMMA proved to be a suitable choice;
- PMMA is easier to bond, when compared to other rather inert thermoplastics such as PE. The microflow elements mentioned above are first molded as open troughs. Gluing a top over the opened side then closes the troughs. The use of suitable glue can become an important issue when chemically inert polymers such as polyolefins (i.e. HDPE) are used for molding, because such polymers are not readily bondable. In contrast to HDPE, PMMA is easy to bond due to its chemical structure that offers active sites for bonding;
- it allows for in situ observation of flow inside microchannels, for embossed parts such as micro heat exchangers and micro DNA separators. The optical clarity of PMMA permits not only direct visualization of the flow, but, in the case of DNA sequencers, it also allows the use of light detectors for determination of changes in the structure of the flow elements;

However, PMMA has a few shortcomings, too:

- PMMA has a shorter elongation at break compared to PE or PC. This can cause problems upon demolding, since the molded microstructures can break inside the metallic pattern before they can be extracted from the mold insert;

- As it was discussed earlier, extended exposure to elevated temperature and pressure leads to stiction. The resulting stiction causes deformation or potential breakage of the molded parts at demolding;
- PMMA degrades relatively easily. When exposed to elevated temperatures, it rapidly generates undesired gaseous monomer. The monomer can create bubbles in the molded part or it can migrate to the surface of the molded part and create superficial dents.

A comparison between selected properties of PMMA, PC, and HDPE is shown in table 3.4. While the tensile strength of PMMA is comparable with PC, the elongation at break is much lower. Together with Young's modulus values that are also different, this suggests that demolding PMMA can be more difficult than for PC.

Table 3.4 Comparison of Selected Properties of Solid PMMA, PC, and HDPE

	64	6	3000	100	70	0.18
	61	115	2200	150	65	0.21
	23	500	1100	-40	200	0.45

Table 3.5 Comparison of Embossing Parameters PMMA vs. PC.
Pattern: DNA Sequencing Chips

	PMMA	PC
Mold Insert temperature, °C	155	180
Substrate temperature*, °C	85	130
Embossing time, min	2	2
Embossing force, N	3800	3800
Force raise rate (0-nom.), N/sec	100	100
Demolding temperature- insert, °C	145	175

(*Measured as temperature of the press platen)

Differences between embossing parameters for PMMA and PC can be seen in table 3.5, which shows sets of values used to replicate a DNA sequencing pattern. The

mold insert temperature is over the Tg for the polymer used. The amount exceeding Tg is less for PC (155-100=55°C) than for PMMA (180-150=30°C) because PC softens more rapidly with temperature than PMMA. The substrate temperature is less than that Tg for both polymers.

3.4.4 Examples of molded patterns: Embossing and manufacture of cross flow micro heat exchanger.

One of the research projects at LSU aims at designing, manufacturing, and testing a micro cross flow heat exchanger. This type of heat exchanger takes advantage of the small scale of the features to make the heat transfer more efficient. By constraining the flow to narrow microchannels, the convective resistance at the solid/fluid interface is reduced, and the heat transfer is enhanced [27]. Also characteristic for these small heat exchangers are the shorter conduction paths through micron-sized walls. These advantages, combined with the fact that these types of heat exchangers have a larger ratio surface area/ volume available for heat transfer, provide for more efficient heat transfer. Ideally, the heat exchanger would be made of a material with very good heat-conduction properties. However, to prove the concept and the design of such a heat exchanger, it was decided to first manufacture it from a polymeric material- PMMA, via hot embossing. The design and assembly of this device are described in detail elsewhere [27]. The mold insert used for manufacture was electroplated as a two-dimensional pattern with features 1000 microns tall and the narrowest gap of 125 microns. A further machining operation turned the mold insert into a three-dimensional pattern, by precision machining of the lines corresponding to the microchannels for liquid flow. Figure 3.3 shows an electron microscope micrograph of the mold insert after machining.

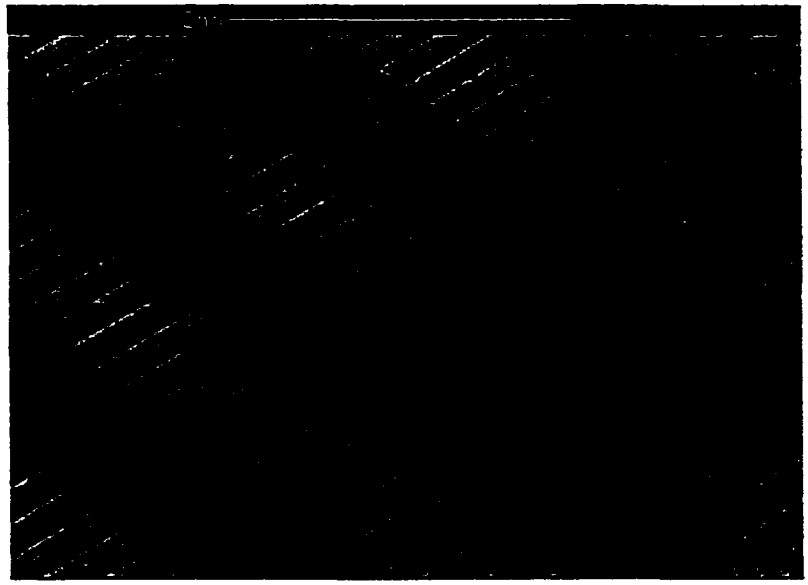

Figure 3.3 Mold Insert for Micro Heat Exchanger

Embossing into the insert shown in figure 3.3 results in replication of one half of the heat exchanger. The complete device is made by assembling face-to-face two such halves, using alignment pins placed around the micropattern.

Issues related to embossing this pattern were the following:

- possible air entrapment;
- stiction due to large lateral contact area between polymer and metal;
- stiction due to undercuts present on the mold insert;
- bowing of the substrate;

As opposed to other mold insert designs, the pattern shown in figure 3.3 has the potential to lead to air entrapment upon embossing. As the metallic microstructures are pushed into the softened plastic, the microgaps between features can become enclosed in plastic and trap air inside. As a result, this pattern is an example where to prevent this from occurring the application of vacuum inside the molding chamber was necessary prior to embossing.

Secondly, the geometry of this mold insert includes a large lateral surface over which the polymer contacts the metal. As it was presented earlier, the adhesion forces developed between the PMMA and the metal are proportional to the lateral contact area. To minimize the stiction, an external mold release agent was used. The mold release has to be applied homogeneously with special care taken to disperse it into the deep and narrow microgaps. The mold release used, having the chemical composition described in the preceding paragraphs, is an aerosol contained in a spray can. It is commercially available as MoldWiz® F-57NC, manufactured by Axel Laboratories, NY. The application was done by spraying at an angle of 45°, from 4 different directions.

As mentioned above, a precision machining operation was necessary to generate the three-dimensional pattern on the insert. The machining was done using a jeweler's saw cutting from the original height of the pattern, along the long lines seen in figure 3.3. This operation caused the top of the machined features to present a burr, sometimes as wide as 75 microns. This undercut was unacceptable for embossing, and it was then necessary to manually remove this burr, using a razor blade, under the optical microscope. Removal of the undercuts together with the use of a mold release minimized the stiction between the substrate and the mold insert. However, when molding the heat exchanger, the adhesion forces are high enough to cause bowing of the substrate when demolding. This bow cannot be relaxed by immediately heat treating the substrate because that would require the patterned side of the 5 millimeters thick substrate to be forced flat, and that would cause distortion of the microstructures. Although it was formed, the bow did not cause problems in the manufacturing steps following embossing. Moreover, the bow was ultimately removed by heat-pressing two

halves against each other, but only after the two halves were thinned down to the final thickness of 850 microns. Figure 3.4 shows a top view of the embossed PMMA part that represents half of the micro heat exchanger.

Figure 3.4 One Side of Embossed PMMA Micro Heat Exchanger

3.4.5 Examples of molded patterns: DNA sequencing chips

Another type of device manufactured via hot embossing are DNA sequencing chips. Several of these patterns are designed by different researchers at LSU, but the general layout is similar to all, and the differences between designs are not significant from the point of view of the molder. The designs have as centerpiece a long microchannel for separation of fluid elements based on differential flow. The channel is typically about 100-200 microns tall and 20-30 microns wide. An example of such a pattern is shown in figure 3.5.

The challenge when embossing such patterns consists in preservation of structural integrity of the fine continuous vertical strip that forms the microchannels. The possibility of deforming the tall and thin (aspect ratios of 6:1) microstructures requires special care when embossing such patterns. As discussed above, successful

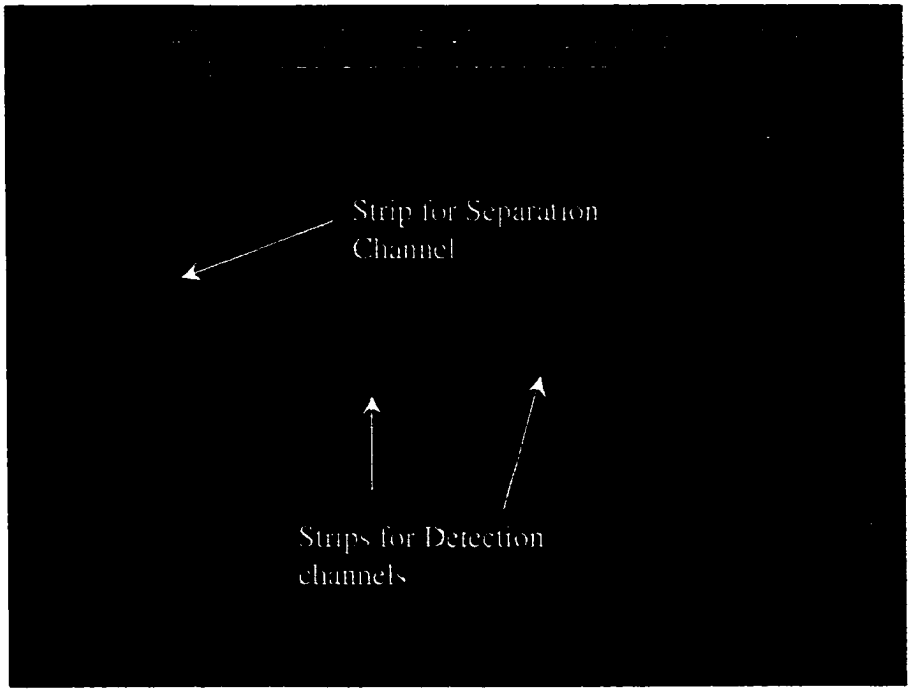

Figure 3.5 SEM Close-up of DNA Sequencing Mold Insert

embossing can be achieved through several combinations of temperature, force, and time, but in a case like this, it is preferable to specifically maximize the temperature and increase embossing time. Doing so allows the insert to be pressed slowly into the soft substrate, protecting the thin microwalls from being deformed. Examples of sets of parameters for embossing DNA sequencing chips were given in table 3.5.

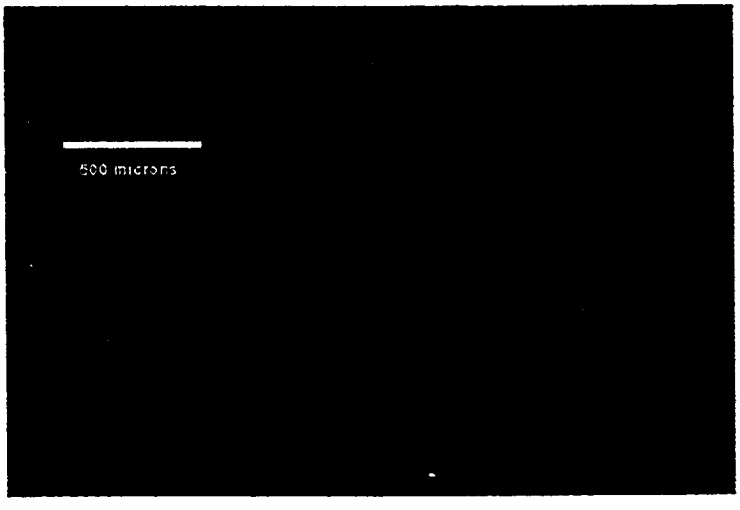

Figure 3.6 SEM micrograph of Hot Embossed DNA Micropattern

A close-up picture of a region on a DNA chip molded in PMMA by hot embossing is shown Figure 3.6. As in discussing injection molding results, the observation is made that the quality of the embossed surfaces depends on the quality of the surfaces of the mold insert.The micrograph in figure 3.7 is a magnified view of the section of DNA chip shown in the preceding figure.

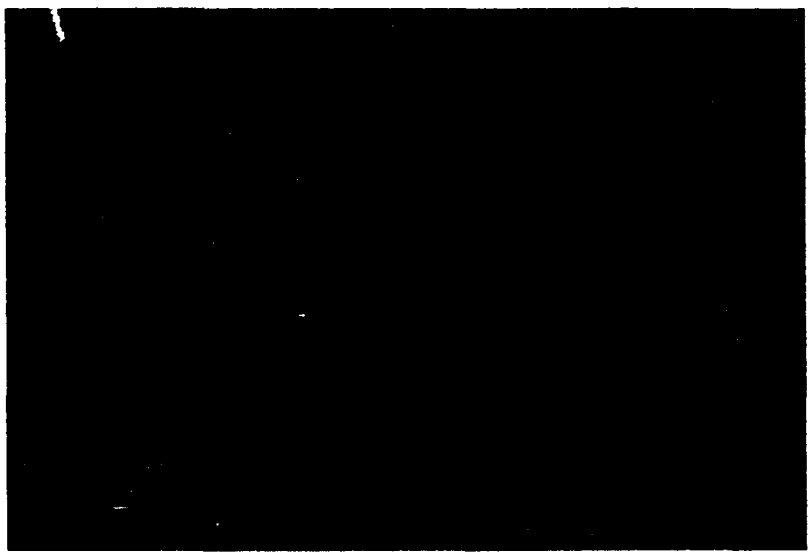

Figure 3.7 Detailed View of Embossed Surfaces

In figure 3.7 it can be seen that the appearances of the top and bottom surfaces of the embossed part are different. This can be explained by the fact that the mold insert used had its surfaces (top and bottom) prepared differently. The bottom surface of the mold insert was polished before electroplating using sandpaper, thus the uneven, scattered marks on the top surface of the molded part. Correspondingly, the top surface of the mold insert was finished by a surface grinding operation, which left parallel marks as seen on the bottom surface of the molded part. As for microreplication of HARMs by injection molding, this observation emphasizes that the mold insert needs to

have a high quality surface finish in order to replicate smooth surfaces on the molded parts.

3.5 Conclusions Hot Embossing

It was shown that hot embossing is a suitable technique for molding HARMs using mold inserts fabricated by LIGA. The embossing machine used is a standard, commercially available parallel-plate press requiring a low initial equipment investment. A vacuum chamber was designed and built to perform the embossing cycle in a below-atmospheric pressure environment. The chamber was designed to accept standard-size mold inserts, readily exchangeable between the hot embossing machine and the injection molding machine. The mold inserts used in the experimental work bear two different patterns; one was used to manufacture a micro cross flow heat exchanger, and the second pattern was used to mold micro flow elements as part of DNA sequencing assemblies. Although the overall cycle time is long compared to the relatively fast cycle time in injection molding, several characteristics of the hot embossing technique make it advantageous for using it in molding HARMs.

First, the operating temperature on hot embossing is relatively low. The hot embossing technique employs a pre-shaped polymer substrate. To pattern this substrate with the desired HARMs design, the molding face of the material is brought at temperatures above the glass transition value. Examples of sets of operating parameters for different mold inserts were given throughout this chapter. However, the technique does not call for the polymer to have a low viscosity, as this requirement exists in injection molding. Consequently, the temperature of operation in hot embossing is less extreme, preventing polymer degradation thus unsatisfactory molding results.

Secondly, the hot embossing technique is gentle on the mold inserts. During the longer cycle times, the operation of the hot embossing press is done by slowly pressing the mold insert into the soft polymeric substrate. As a result, the chances to deform the fragile tall and narrow microstructures are minimized. From the experience accumulated in this work, after over 100 embossing cycles the quality of the molded parts has been preserved at the original standards. At the conclusion of this work, both the heat exchanger and the DNA sequencing-type mold inserts have preserved the original geometry and are scheduled for continuous use in future molding cycles.

A third advantage of hot embossing is also related to the imposed long cycle time. Slow operation corresponds to low deformation rates of the polymer substrate. This not only protects the structural integrity of the mold inserts but it also promotes molding of stress-free parts. It was discussed that by employing long experimental times, the value of the Deborah number is maintained low, and the polymer is then allowed to relax and to conform to the surface of the metallic mold insert.

It was also shown that the hot embossing technique is sensitive to the quality of the molding substrate and the quality of mold inserts. The PMMA substrates need to be conditioned prior to molding, as the presence of moisture causes low-quality parts to be embossed. Also, it was concluded that the surface definition for the molded part matches the finest imperfections present on the mold inserts. Because hot embossing results in accurate reproduction of all details, the mold insert needs to be manufactured with a high surface finish.

CHAPTER 4. COMPARATIVE STUDY HOT EMBOSSING VS. INJECTION MOLDING

4.1 Design of Experiments

Several aspects of injection molding and hot embossing for LIGA were presented in the previous chapters. In this chapter, a comparison between the two techniques is presented. The comparison was done through a set of molding experiments designed and executed using two mold inserts both in injection molding and in hot embossing.

The planning of the experiments started with the design of the mold insert pattern. First, it was decided to investigate the effect that the microstructure *height* will have on the outcome of the molding process. It was expected that taller or deeper microstructures would pose more challenges when molding, due to an increase in vertical aspect ratio. To study that effect, it was planned to manufacture two different mold inserts, having heights of 200 and 500 microns, respectively. Consequently, the first factor in the experimental design is mold *height*.

Next, the effect that the lateral aspect ratio would have on the outcome of the molding process was considered. At the same height, the comparison between different lateral aspect ratios is done between microstructures which have one side length in common or between microstructures that have different side lengths but the same footprint. Qualitatively, this translates in comparing "short", "long", and "wide" microstructures among each other. When increasing the lateral aspect ratio by increasing the length of either one or both sides of a microstructure, the vertical sides of the microstructure increase in area, which means that the contact surface between plastic and metal is increased. This also corresponds to an increase in the support area

for the molded microstructure, but at different rates depending if one or both sides are lengthened. The ratio between the area of the vertical sides (A_v) and the area of the footprint (A_c) is:

$$\frac{A_v}{A_c} = \frac{2h(l+L)}{lL} = 2h\left(\frac{1}{l} + \frac{1}{L}\right)$$

where l is the width of the microstructure, L is the length, and h is the height. Assuming tensile failure only, when separating the molded part from the metallic insert the stiction forces are opposed by the tensile strength of the microstructure:

$$F_s = \sigma_p A_c$$

but

$$F_s = \tau_v A_v$$

where σ_p is the plastic tensile strength and τ_v is the shear stress at the polymer/metal interface. This shows that, for given values of σ_p and τ_v, the ratio A_v/A_c dictates the behavior of the microstructure upon demolding. It was decided for each of the two inserts (each height), that the pattern should include two types of features: square features and rectangular features. The square features have two different side lengths, 40 and 160 microns, while the rectangular features have the dimensions 40x640 microns and 160x2560 microns. This results in four possible levels for the *shape* factor.

Rewriting the A_v/A_c ratio in terms of the basic length l_0=40 μm yields:

$$\frac{A_v}{A_c} = \frac{2}{l_0} h\left(\frac{1}{x} + \frac{1}{y}\right) = \frac{2h}{l_0} R$$

where $R = \left(\frac{1}{x} + \frac{1}{y}\right)$. The values of the *(x;y)* pair are as follows: (1:1), (1:16), (4:4), (4:64). A plot of the A_v/A_c ratio versus the cross-sectional area of the microstructure (footprint) is shown in figure 4.1. In addition, all four shapes were designed to be

electrodeposited both as positive features (posts) and as negative features (holes). By doing so, the third factor of the design was introduced as *tone*, with two levels.

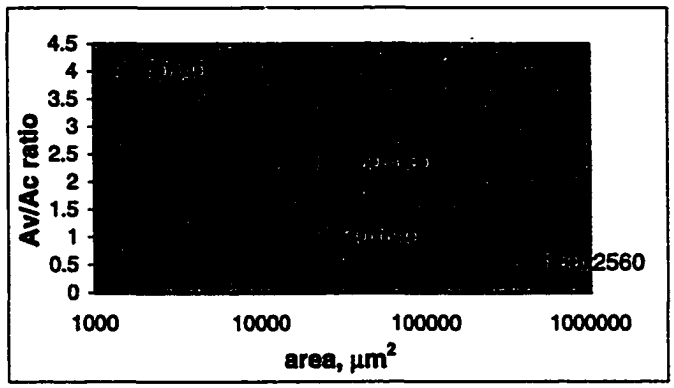

Figure 4.1 Plot of *Av/Ac* Ratio Versus Cross-Sectional Area, 200 μm Mold Insert

Finally, each type of feature, for instance a 200 microns tall rectangular 40x640 post was made in six replicas that were spaced a certain distance apart. The spacing was the same for all types of features. Thus, the last factor introduced in the study is *spacing*. Three different values of spacing were prescribed: 40 microns, 160 microns, and 640. A drawing of the pattern is shown in figure 4.2, with the negative features at the top half and the positive ones at the bottom half. The drawing is to scale.

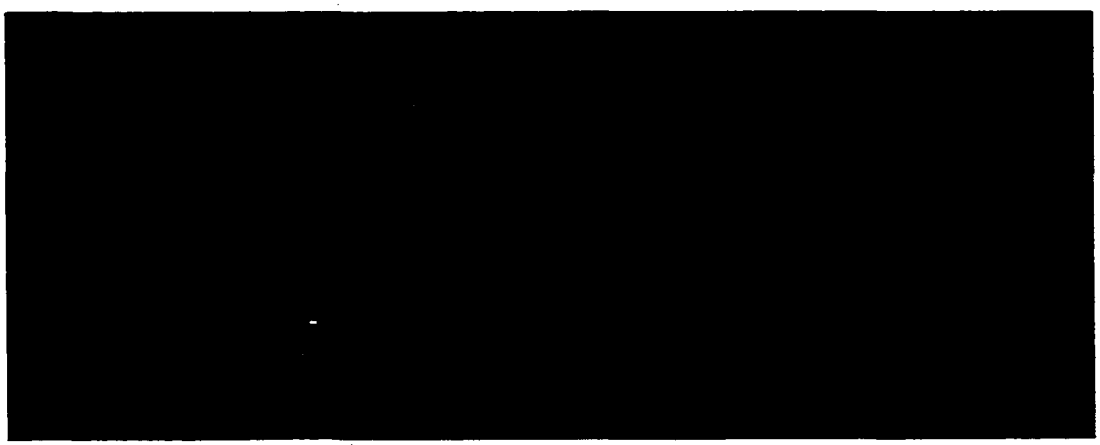

Figure 4.2 Design Layout for Test Mold Insert

4.2 Mold Insert Making

The mold inserts were fabricated using LIGA. The design pattern was first transferred from a graphical drawing to an optical mask using the pattern generator at CAMD. The optical mask was then used to pattern an x-ray mask, using the UV-light source in the Electrical Engineering Dept., LSU. The x-ray mask was made using a Kapton® membrane, with gold as the x-ray absorber. Next, the x-ray mask was used to pattern two different PMMA substrates, with heights 200 and 500 microns, respectively. The substrates were first glued onto conductive support plates: the 200 microns PMMA was glued onto a 4¾" stainless steel plate and the 500 microns PMMA was glued onto a 4¾" titanium plate pretreated with a thin layer of TiO_2. The two support plates are made of different materials because two different mold-making techniques were employed when electrodepositing nickel, as it will be discussed later. The two PMMA substrates, now glued onto their respective base plates, were patterned using x-rays from the CAMD synchrotron. The x-ray exposure was done through the x-ray mask and an aluminum filter, using 1.5 GeV radiation, with a bottom dose of 3500 J/cm^3. The PMMA substrates were then developed to remove the exposed polymer, and the resulting pattern was ready for use as template for electroplating. The electrodeposition of both mold inserts used a nickel sulphamate solution. The plating bath included, besides the plating salt, boric acid (as pH buffer) and lauryl sulfate (as wetting agent). The electroplating was carried out galvanostatically, at 20 mA/cm^2, and 55°C. On one hand, the 200 microns insert was produced by electroplating nickel from the stainless steel face up and just over the height of the PMMA template. The electroforming step was then followed by a surface grinding operation performed to remove the "over-

plated" excess material. After surface grinding, the top surface of the mold insert was finished in a polishing operation. The polishing was done to remove the burrs resulting from the rougher mechanical abrasion of the nickel. The polishing operation was done using two polishing suspensions, 5 micron particle size silicon carbide, followed by 1 micron particle size alumina. Alternately, the 500-micron tall mold insert was made by plating on titanium oxide, again exceeding the height of the PMMA substrate, but now running the electroplating process for 10 days after the first over-plating was formed. This led to the formation of a thick deposit on top of the PMMA template. This thick deposit became the base plate of the 500 tall micropattern, because the original titanium plate, which served as plating substrate, was later removed by simply prying it from the overplated nickel. This separation was possible because the Ti surface had been pre-treated with an oxide layer, thus creating an electrically conductive but mechanically weak interface between the Ti base plate and the Ni deposit. After separating the electroplated nickel from the Ti plate, the overplated surface was planarized by a face milling operation.

Table 4.1 Sample Measurement Data for 500 micron Mold Insert

2560	160	500	1	1	2559	161	536
2560	160	500	1	1	2560	160	552
2560	160	500	1	1	2560	162	544
2560	160	500	1	1	2561	161	548
2560	160	500	1	1	2563	162	544
2560	160	500	1	1	2558	162	547

The resulting mold inserts were measured using an optical microscope coupled with a stage displacement measurement system and a digital camera. Measurements

were taken for the height, length and width of each individual microfeature, resulting in 144 features measured per insert, and a total 864 height, length and width measurements for both inserts. A sample from the measurements data set is shown in table 4.1.

4.3 Molding Experiments

Hot embossing and injection molding were used to replicate the pattern on the two test mold inserts. In both instances, the molding was performed using PMMA, pre-shaped as 5.3"disks in the case of embossing and as pellets in the case of injection molding. The values of the operating parameters for each technique are given in tables 4.2 and 4.3.

Table 4.2 Example of Embossing Parameters. Pattern: Test Molding. Embossing Substrate Material: PMMA Max. Aspect ratio: 500:40

Mold Insert temperature, °C	180
Substrate temperature*, °C	85
Embossing time, min	3
Embossing force, N	3800
Force raise rate (0-nom.), N/sec	100
Demolding temperature- insert, °C	145
Demolding temperature- substrate*, °C	45

(*Measured as temperature of the press platen)

Table 4.3 Example of Injection Molding Parameters. Pattern: Test Molding. Embossing Substrate Material: PMMA Max. Aspect ratio: 8:1

Mold Insert temperature, °C	180
Melt temperature*, °C	280
Melt Flowrate, cm^3/s	10
Holding Pressure, bar	150-300
Holding time, s	40
Demolding temperature, °C	100

* at nozzle

The success rate of the molding process was limited. Some features were molded in both heights and with both methods, while some features could not be

produced using both techniques or both mold inserts. Some features could not be produced at all. Table 4.4 summarizes the success rate of the molding experiments by molding method, insert size, tone, feature width and length, and spacing. The light gray cells are combinations that did not exist as microfeatures on the respective mold inserts before molding due to imperfections in the mold insert fabrication process. The cells with white background represent positions where molding was not successful. The cells with darker background represent combinations that were molded successfully.

Table 4.4 Results of Injection Molding and Hot Embossing Experiments

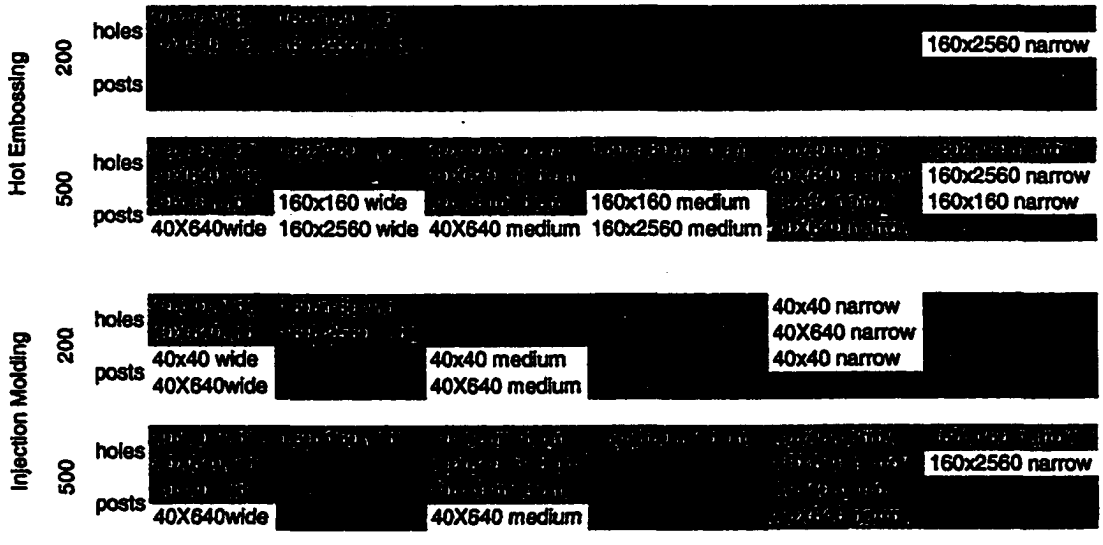

Qualitatively, the results in table 4.4 indicate that the molding of PMMA into the test pattern under discussion was different with regard to mold insert height. The success rate for the 200 micron mold insert is higher than the 500 micron insert, both for injection molding and for hot embossing. As it was presented earlier, the higher (or deeper) microstructures appear to have been more difficult to be replicated. When unsuccessful results for the 200 micron and the 500 micron mold inserts are pooled together per molding method, table 4.4 indicates that the success rate may be regarded as insensitive to the molding method used, either hot embossing or injection molding.

However, a closer look suggests that hot embossing worked better for the 200 micron insert, while the 500 micron insert was easier to replicate using injection molding.

Several reasons can be listed to explain this difference between the embossing results and the injection molding results. The list includes the geometry of the mold inserts at the top, the difference between the rate of demolding in embossing versus injection molding, and the existence of a different thermal regime based on different characteristic dimensions for each type of microstructures. Also, the temperature field across the mold insert when mounted onto the embossing machine was probably different versus when mounted in the injection machine.

The top of the mold inserts was examined using a scanning electron microscope. It was believed that the two inserts had a different appearance at the top, since the electroplating/polishing were performed differently for each insert. Indeed, SEM observation of the mold inserts revealed different topographies for the two mold insert tops. The 200 micron mold insert, because it was only slightly overplated, and the overplating had to be lapped down by surface grinding, presented a more pronounced overhang (burr) due to this harsh mechanical abrasion, despite the final polishing operation that was performed on that surface. This imperfection (burr) was measured to be around 2-3 microns wide, which made it sizeable when compared with characteristic widths of 40 microns. Two photographs of the overhang, including the estimate measurement are shown in figures 4.3 and 4.4.

The image in figure 4.3 shows a 40x640 micron positive feature with a considerable overhang at the top. The picture was taken after the molding experiments were complete. It can be seen that the overhang appearance is rounded, indicating that

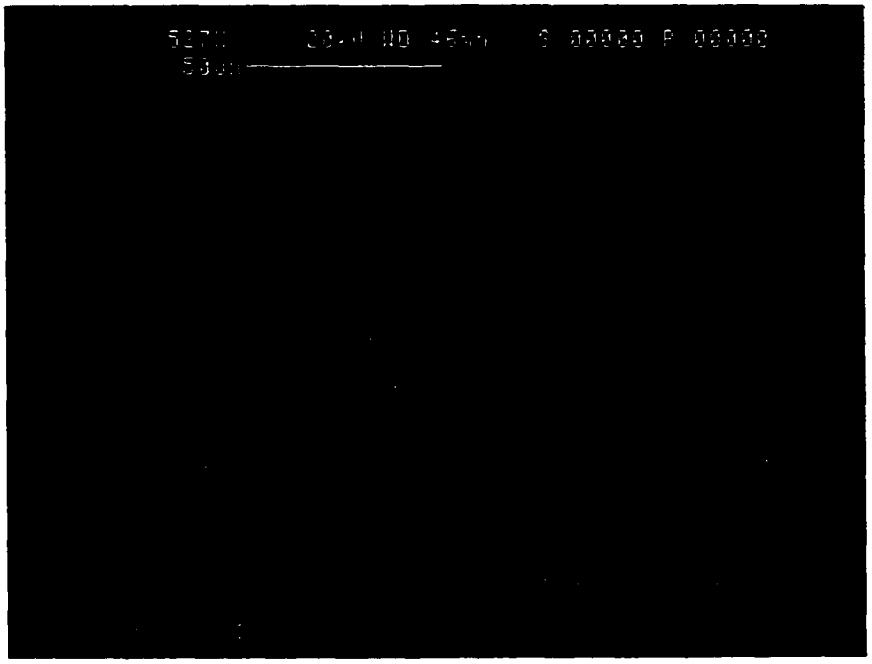

Figure 4.3. SEM Micrograph of 200 micron Microfeature- Top View

the molded plastic features did not break the overhang upon demolding, but the burr was bent upwards. Also noticeable are the estimate measurements of the overhang, shown in figure 4.4. The measurements were taken on a 40x640 micron type feature. Highlighted at the top of the two pictures are the widths measured between the vertical lines. It can be seen that the size of the overhang is very large compared to the characteristic width of 40 microns. For the 500 micron mold insert, the manufacturing process did not involve overplating followed by surface grinding. As a result of the way the insert was made, the electroplated microfeatures did not present a sizable overhang resulting from mechanical abrasion of the top. A small overhang was, however, noticed under the SEM, consisting of TiO_2 crystals that broke with the Ni plating away from the Ti plating substrate. The size of the overhang for the 500 micron insert was estimated to be at submicronic level, much smaller than for the 200 micron mold insert.

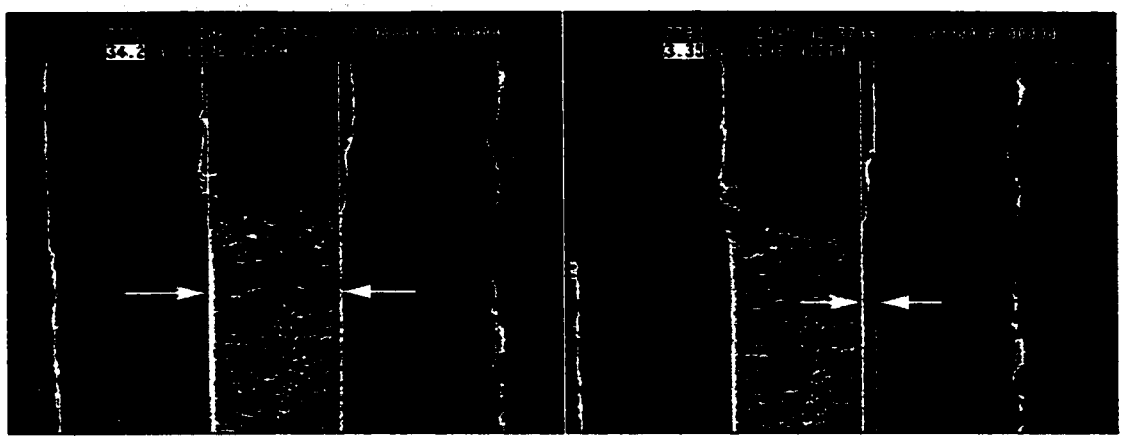

Figure 4.4. SEM Micrograph of 200 micron Estimated Overhang Width

The explanation for the different success rates for injection molding and hot embossing relative to the two mold insert heights could also be found in the demolding step. When the mold insert is separated from the molded plastic part, the molded microstructures are subject to tension forces due to stiction and overhang. Relative to the rate of separation, the dynamic response of the polymeric material can consist of a more plastic behavior for a slower rate and more elastic behavior when a faster, more brisk rate of separation is imposed. It is believed that the demolding mechanism in hot embossing facilitated the extraction of shorter (200 microns) features from their corresponding microgaps, despite the presence of the overhang. By separating the two surfaces very slowly, the polymer was allowed to elongate and slide over the overhang, and out from the microgap. At the same time, the strength of the plastic feature overcame the stiction forces that are proportional to lateral surface area. In contrast, the lateral surface area for the 500 micron insert was large enough to cause the stiction to exceed the strength of the plastic microfeature, causing them to break despite the slow separation rate. The opposite is believed to hold true for the injection molding. There, the demolding was performed at a higher rate, which favored the extraction of the 500

micron features. The rapid separation of the mold insert caused the polymer to respond in an elastic, stiff manner, overcoming the stiction to the lateral surface. In contrast, the rapid separation did not benefit the 200 micron features, where the overhang caused a sizeable change in cross section; decreasing the total strength of the polymeric features and causing them to break more often than the 500 micron ones. An example of a field of molded 200 micron microposts is shown in figure 4.5.

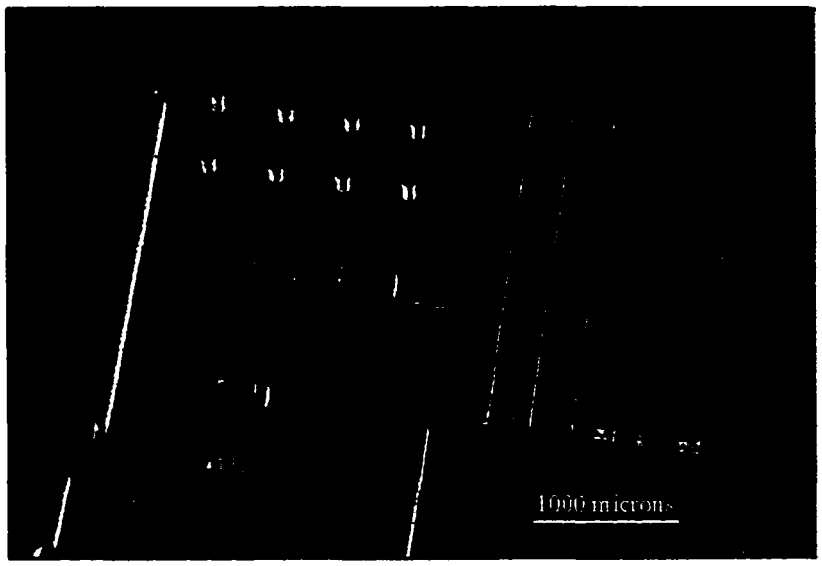

Figure 4.5 Field of 200 Micron Embossed Microfeatures

One of the goals of this set of experiments was to quantify the shrinkage that the plastic microstructures undergo during micromolding. To determine the shrinkage value, the molded plastic parts were measured using the optical system setup described before. Each individual microfeature was measured for height, width and length

Width, length, and height measurements taken on the plastic parts were compared to the same corresponding dimensions on the mold inserts into which the molding was done. This comparison was reported as a percent change in dimension:

$$\%change = 100 \cdot \left(\frac{dim_{mi} - dim_{p}}{dim_{mi}} \right)$$

where dim_{mi} is the dimension on the mold insert and dim_p is the measurement on the molded part. Consequently, 288 microfeatures were measured, 72 per insert/technique combination. From this total, most values for height and width %change were negative, and could not be used in reporting an overall shrinkage value. Measurements for plastic posts with positive percent values for width and length were grouped together resulting in a smaller data set. For this data, the height shrinkage values (some positive, some negative) were averaged based on the cross sectional geometry. Table 4.5 summarizes the information based on the cross-sectional area of the microposts.. Percent-change values are reported: also reported in the same table are the values of the Av/Ac ratio, as plotted in figure 4.1. The data in these two columns are plotted together in figure 4.6.

Table 4.5 %Change for Height and Av/Ac Ratio

40x40	1600	-3.91	4
40x640	25600	-3.21	1
160x2560	409600	-2.15	0.5313
160x160	25600	-4.71	2.333

As discussed above, the *Av/Ac* ratio is proportional to the ratio of stiction forces and tensile strength for a given microstructure. For plastic posts, this ratio is therefore a predictor of the ease with which microstructures of a given geometry will separate from the metallic insert (demold). The comparison of the percent change in height and the *Av/Ac* values is then justified by the fact that the elongation of microstructures is a direct result of its tensile response to stiction forces.

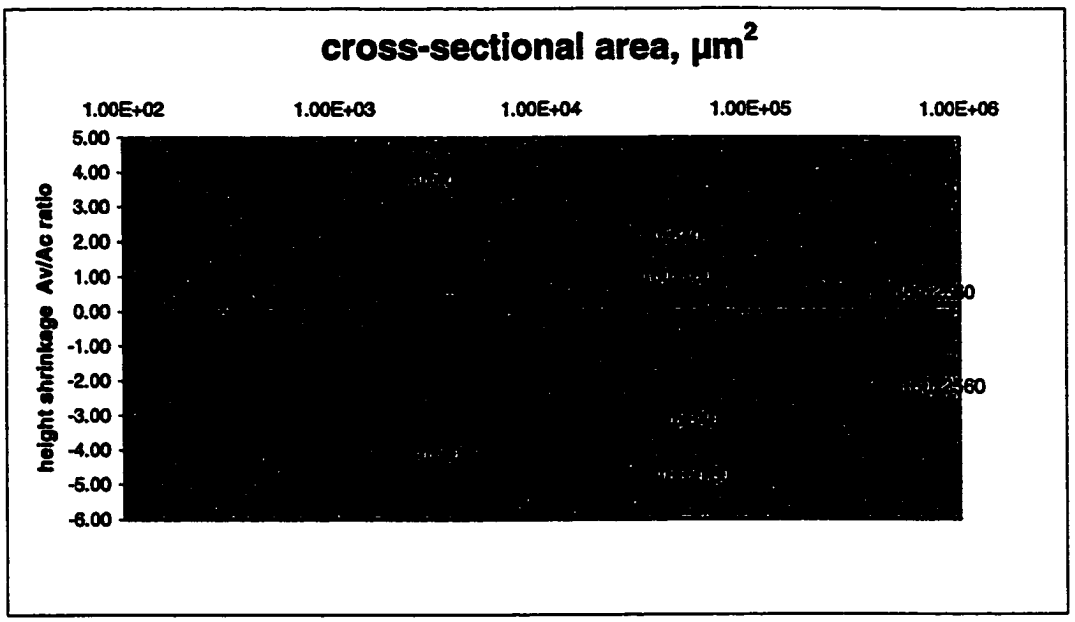

Figure 4.6 %Change Height and Av/Ac Ratio vs. Cross Sectional Area

An enhanced adhesion between plastic and metal causes the plastic microstructure to elongate before being demolded from the insert. Values for the *Av/Ac* ratio shown in figure 4.6 predict that the more difficult separation thus the greatest elongation will occur with the 40x40 micron features, followed by the 40x640, 160x160, and 160x2560 features. As predicted by the *Av/Ac* values, the 40x40 microfeatures did exhibit a high degree of elongation, while the 160x2560 features exhibited the lowest. The intermediate values of 40x640 and 160x160 have reversed positions on the %change plot, when compared to the *Av/Ac* values. Also, these values appear slightly shifted towards higher percent-change relative to the 40x40 features. This could be explained by the material properties of the polymer at the time of demolding. Since the narrower 40x640 features cooled down faster than the wider 160x160 ones, the polymer was at a higher temperature in the latter case, thus it exhibited greater elongation than expected when demolded from the insert. Based on

the same explanation, the 160x2560 microstructures probably had larger elongations than the *Av/Ac* values predicted.

Last, but not least, a set of 24 measurements, all with positive %change values, were averaged for width, length, and height. The averaged values are reported in table 4.6. These values represent the percent change of the corresponding dimension of the plastic part due to thermal shrinkage, only. As seen, these values are homogeneous around an overall mean of 1.26%.

Table 4.6 Average Shrinkage Values for LIGA molded HARMs

1.73	0.96	1.07

4.4 Conclusions on Comparison between Injection Molding and Hot Embossing

Experiments were planned and performed to compare hot embossing and injection molding for LIGA HARMS. Two mold inserts bearing the same test pattern were manufactured in two different heights, 200 and 500 micron. The mold inserts were manufactured using LIGA: the 200 micron insert was plated on a stainless steel substrate and the 500 micron insert was manufactured by overplating and debonding from the original Ti substrate. The overplating was later machined flat to become the mold insert base. The test pattern on the mold inserts was designed to measure the influence of height, width, length, spacing and tone on the dimensional change of the molded plastic microfeatures. The molding experiments yielded mixed results: some microstructures were molded properly, while others were elongated or broke upon demolding. The successfully molded microstructures were measured for height, width, and length and percent change in these dimensions were calculated. The number of observations gathered was insufficient to perform a complete statistical analysis on the

influence of all factors above-mentioned. However, average shrinkage values could be and were calculated for the features that were molded correctly. The reported mean value for the shrinkage was 1.25 %. This value could be used as a design guide when planning micropatterns that require a high degree of control over the dimensions of the final molded part. Qualitative interpretation of the molding results was also done. It was shown that the success rate for the 200 micron mold insert was higher than that for the 500 micron insert, both for injection molding and for hot embossing. This was assessed based on the total number of features molded successfully. Also, the molding results suggested that hot embossing worked better for the 200 micron insert, while the 500 micron insert was easier to replicate using injection molding. This difference was explained based on the demolding step following immediately after molding. It was argued that the difference in the dynamic loading of the polymer upon demolding could offer the explanation for this relationship.

CHAPTER 5. FINAL CONCLUSIONS AND RECOMMENDATIONS

The advent of LIGA is "old news" at the time this work is being written. The research presented in these pages started with small steps representing some of the earliest systematic efforts in the US in the field of LIGA and more specifically, molding for LIGA. Since then, more and more groups have been involved in the development and application of LIGA for research purposes and, more recently, for commercial use. Applications of LIGA-manufactured micro components have been marketed or are currently under development in fields including biomedicine, sensors, actuators, heat transfer, optics, etc. Moreover, some of the results presented here are currently applied in the daily activities of a start up company created based on the research work from LSU's Microsystem Engineering Team. These developments serve as proof that LIGA is viewed as a promising technology, which can compete in the market for technologies used for fabrication of large-area parts covered with micro features.

Molding is the last step in the LIGA manufacturing sequence. Molding gives LIGA the mass-production character, allowing for production of low-cost parts. The two molding techniques investigated in this work were injection molding and hot embossing. Both techniques proved to be suitable for use to reproduce layouts of micropatterns existing on mold inserts manufactured by x-ray exposure of PMMA and electroplating in the so-produced PMMA templates. The molding research work was based on two commercially available machines. While the 150-ton injection machine was already in place before the beginning of the research, the parallel-plate press was purchased at the start of the investigative efforts in the area of microreplication by hot embossing. Preliminary experiments with both machines indicated that several

modifications and additions were necessary to adapt the injection machine and the embossing press for microreplication. For the injection machine, the manufacture of a suitable mold was pursued including the addition of a vacuum system (needed to evacuate the air out of the mold cavity prior to injection of the polymer melt), and the design and manufacture of a heating/cooling system for the mold. Several technical solutions were investigated for the design of the mold, until a final geometry was adopted, in relationship with the specific requirements for molding PMMA, as presented in chapter 2. The resulting mold geometry ensures minimal pressure loss upstream from the entrance into the mold cavity, together with optimal shape for molding and demolding PMMA parts.

For the hot embossing press, a vacuum chamber was designed and built to fit between the press platens. The vacuum chamber contains the embossing sandwich, with the temperatures of the mold insert and of the substrate controlled through the press' heating/cooling system. The mold for injection molding and the vacuum chamber for the hot embossing press were designed to accept the same standard-size mold inserts. This allows for rapid interchange of mold inserts between the two molding machines.

Experiments were performed to identify the important process parameters in injection molding of HARMs-patterned mold inserts. It was established that the temperature of the mold insert is of primary importance for the process, followed by the melt flow rate. For the process of hot embossing, it was argued that changes in the temperature of the substrate have most evident effects on the process, followed by variations in the embossing force and embossing time. It was shown that the embossing

time should preferably be long, to allow for relaxation of the macromolecular chains resulting in stress-free moldings.

Regarding the materials for molding, several thermoplastics were used throughout the experiments. Injection molding was studied using mainly two polymers: high density polyethylene- HDPE and polymethylmethacrylate- PMMA. Compared to HDPE, it was shown that PMMA is heat-sensitive, and that it requires special care including drying before dosage, and dosage under controlled temperature and shear conditions to prevent molecular degradation. When used in hot embossing, PMMA is advantageous compared with polycarbonate- PC, because it allows embossing at lower temperatures. While thermal degradation of PMMA can be avoided more easily in hot embossing, moisture content still needs to be kept minimal for proper part quality. PC was used as an alternate embossing material for PMMA. PC also has good optical properties and is easy to machine and bond. Moreover, its higher glass transition allows parts molded from PC to be used at temperatures higher than Tg for PMMA, without softening or deformation of the part. Also related to molding materials, it was noted that successful molding consists of fully penetrating into the microgaps on the mold insert and also proper demolding of the plastic microstructures from the metallic pattern.

Molding experiments presented in this work confirmed previous research, which indicated the importance of using a proper demolding agent to facilitate the separation of the plastic part from the metallic insert. Two demolding agents were used: a silicon-based spray for HDPE, and a mix of phosphate esters, polyolefins, and fluoropolymers for PMMA and PC.

Several patterns were molded during this research work. Molding of various new patterns was improved and made faster by the design of standard-size mold insert geometry. From inception of this work, three micro heat exchanger geometries were molded (and fabricated for testing), one stacked pattern and two cross flow patterns. Also, several DNA sequencing chips were microreplicated, using both injection molding and hot embossing.

The last pattern to be replicated in both molding machines was a test pattern. This pattern was designed for comparison between techniques performed by molding into two inserts of different heights (200 and 500 microns) using the same material (PMMA). Insufficient number of measurements of molded microfeatures could not provide enough data for a comprehensive statistical analysis to be performed. However, by measuring all microfeatures molded correctly an overall mean value of 1.25 % was reported for shrinkage of the plastic compared to the mold insert. This value can be used as a design guide when planning PMMA micropatterns that require a high degree of control over the dimensions of the final molded part. Qualitative interpretation of the molding results showed differences in the demolding success rate between the two molding techniques combined with the two mold insert heights. These observed differences were used to emphasize the importance of mold insert quality on the microreplicated part, molded using either injection molding or hot embossing.

As a last consideration to be made at the end of this work, the author believes that the question "which method is better for microreplication: injection molding or hot embossing?" does not have a definitive answer. Both methods work, and both methods present advantages and disadvantages when compared to each other. As discussed

throughout this work, the selection of one method over the other depends on what is to be molded, in what material, and on how fast and accurate does the microreplication need to be. Injection molding is a faster technique, but the molding material is processed under high temperatures and shear rates, which can lead to the chance of molecular degradation and can leave the part with frozen-in stresses after demolding. Hot embossing is more attractive for use when sensitive polymers such as PMMA are to be used, because it avoids the above-mentioned shortcomings. However, it is less advantageous as a large-scale manufacturing technique due to its longer cycle time.

The recommendations for future work start with this last consideration. A systematic study of the stresses induced by either technique will illustrate the difference between the qualities of the molded products made using each technique. The stressed regions in the molded microstructures are most likely found at the polymer-metal interface, and would probably be best-detected using optical or electron microscopy techniques.

A second suggestion for future research would involve the study of the flow of the polymer inside the microstructures on the mold insert, for both injection molding and hot embossing. This study would better define the influence of operating parameters on the molding process, helping to set proper values for accurate control of injection molding or hot embossing. This study would involve numerical simulations for the flow, coupled with measurements of pressure and temperature distributions along the flow path.

REFERENCES

1. Ruprecht R., Kalb H., Kowanz B., and Bacher W., Molding of LIGA Microstructures from Fluorinated Polymers, Microsystem Technologies 2 (1996) 182-185

2. Bacher W., Menz W., and Mohr J., The LIGA Technique and Its Potential for Microsystems-A Survey, IEEE Transactions on Microelectronics, vol 42 no 5, October 1995;

3. Becker, E.W., Ehrfeld, W., Munchmeyer, D., Betz, H., Heuberger, A., Pongratz, S., Michel H. J., and Siemens, V.R., Production of Separation Nozzle for Uranium Enrichement by a Combination of X-Ray Lithography and Galvanoplastics, Naturwissenshaften, vol 69, 1982, p. 520-523;

4. Fasset J., Thin Wall Molding: How Its Processing Considerations Differ From Standard Injection Molding, Plastics Engineering, December '95, 35-37;

5. Christenson T. R., and Guckel H., Deep X-Ray Lithography for Micromechanics, SPIE Proceedings of Micromachining and Microfabrication Process Technology, 23-24 October 1995, Austin, Texas;

6. Ehrfeld W., Abraham M., Ehrfeld U., Lacher M., and Lehr H., Materials for LIGA Products, Proceedings IEEE Micro Electro Mechanical Systems, Oiso, Japan, January 25-28, 1994;

7. Ehrfeld W., Bley P., Gotz F., Hagmann P., Maner P., Mohr A., Moser J., Munchmeyer H. O., Schelb W., Schmidt D., and Becker E.W., Fabrication of Microstructures using the LIGA, presented at Micro Robotsand Teleoperators Workshop, Hyannis, Massachusetts, 1987;

8. Kelly, K., Stephens, S., Kountouris, D., McLean, J., Coynel, J., "Construction and Testing of a Micro Heat Exchanger on the End Face of an Annular Ring", submitted to the Journal of Microelectromechanical Systems, December 1998.

9. Stephens, S., Kelly, K., Kountouris, D., McLean, J., Coynel, J., "Application of Micro Heat Exchangers to Turbomachinery Components", submitted to the Journal of Microelectromechanical Systems, December 1998.

10. Madou, M., Fundamentals of Microfabrication, Preprints, Chapter 5: Surface Micromachining;

11. Harmening M, Bacher W., Bley P., El-Kholi A., Kalb H., Kowanz B., Menz W., Michel W., and Mohr J., Molding of Threedimensional Microstructres by the LIGA Proces, Micro Electro Mechanical Systems '92, Travelmünde, Germany, February 4-7, 1992;

12. Ruprecht R., Bacher W., Haußelt J.H., and Piotter V., Injection Molding of LIGA and LIGA-Similar Microstructures using Filled and Unfilled Thermoplastics, Proceedings at the SPIE Micromachining and Microfabrication Process Technology, 23-24 October 1995, Austin Texas;

13. Breuer P., Microinjection Molding From CDs to Implants, Miniature Parts are Key to Developing Microsystems, Modern Plastics, Mid-November 1995 d84-D85;

14. Rahner S., and Neilley R, Microparts: Market growing, Parts Shrinking, Injection Molding, October 1998, 150-152;

15. Arburg Allrounder® CMD with Dialogica® Control, User's Manual

16. Despa, M., Injection Molding of High Aspect Ratio Microstructures, A Thesis, Louisiana State University, May 1998

17. Rosato D.V. and Rosato D. V., Injection Molding Handbook, Second Edition, Chapman & Hal, 1995;

18. Vardeman, S. B., VanValkenburg, E. S., Two-way Random Effects Analyses and Gauge R&R Studies, Technometrics, August 1999, Vol. 41, No.3;

19. Becker H., Heim u, Polymer High Aspect Ratio Microstructures Fabricated with hot embossing, Jenoptik Mikrotechnik Technical Report

20. Madou, M., Fundamentals of Microfabrication, Chapter 6:LIGA, CRC Press, 1997;

21. Xia Y., McClelland J. J., Gupta R., Qin D., Zhao X-M., Sohn L., Celotta R. J., and Whitesides G. M., Replica Molding Using Polymeric Materials: A Practical Step Toward Nanomanufacturing, Advanced Materials, No. 2, 9, 1997

22. Bird R. B., Stuart W. E., and Ligtfoot E. N., Transport Phenomena, John Wiley & Sons, 1960;

23. Bley P., Menz W., Bacher W., Feit K., Harmening M., Hein H., Mohr J., Scomburg W. K., and Stark W., Application of the LIGA Process in Fabrication of Three-Dimensional Mechanical Microstructures; Proceedings of 1991 International MicroProcess Conference, 384-389;

24. Both A., Bacher W., Heckele M., Muller K.D., Ruprecht R., and Strohmann M., Molding Process with High Alignment Precision for the LIGA Technology, Proceedings IEEE Micro Electro Mechanical Systems, Amsterdam, the Netherlands, February2, 1995;

25. Tadmor Z. and Gogos C.G., Principles of Polymer Processing, John Wiley and Sons Inc, 1979;

26. Jenoptik Mikrotech GmbH Inetrnet Webpage, http://www.jo-mikrotechnik.com/english/index.html;

27. Harris C., Despa M., and Kelly K., Design and Fabrication of Cross-flow Micro Heat Exchanger , Journal of MEMS, Vol. 9, December 2000.

VITA

Mircea was born on August 18th 1969, in Ploiesti, Romania. Between 1983 and 1987, he was enrolled at the "Mihai Viteazul" high school, in the mathematics and physics section. During the same time, he played team-handball at the "C.D. Gherea" sports club and became national vice-champion in 1984.

In July 1987, he was admitted at the "Politechnica" University of Bucharest. Before starting college, he served in the Romanian Army for the required 9 months of military service. Then, he enrolled as a freshman in September 1988. He married Simona in November 1992. In July 1994 he graduated from U.P.B with a degree in Chemical Engineering with concentration in Polymer Science.

After graduation, he was accepted a position as a research engineer at the National Romanian Oil Institute. He maintained the same position until his departure to Louisiana State University.

Mircea enrolled as a graduate student in the Department of Chemical Engineering at L.S.U. in August 1995. His research focused on the manufacture of microstructures and their replication by plastic molding. After defending his thesis in 1998, he continued to work towards his doctorate degree with Dr. Kevin Kelly as graduate advisor. In May 2001, he will be conferred the degree of Doctor of Philosophy.

DOCTORAL EXAMINATION AND DISSERTATION REPORT

Candidate: Mircea S. Despa

Major Field: Engineering Science

Title of Dissertation: Molding Large Area Plastic Parts Covered with HARMs

Approved:

Major Professor and Chairman

Dean of the Graduate School

EXAMINING COMMITTEE:

Date of Examination:

December 4, 2000